# El Niño-La Niña events

# simulated with Cane and Zebiak's model

# and observed with satellite or *in situ* data. Part 2: model forced with observations

by

Boris Dewitte and Claire Perigaud

submitted to Journal of Climate

25 July, 1994

address:

CALTCH / Jet Propulsion Laboratory, MS 300/323, 4800 Oak Grove Drive, Pasadena.

CA 91109- USA

## ABSTRACT

In this paper, we examine the conditions under which the Cane and Zebiak's model can be run so that the simulated anomalies of wind and SST agree better with the observations. When forced with observed SST, the atmospheric model simulates wind anomalies in much better agreement with observed winds. The simulated winds, however, are located too close to the SST anomalies in the east. The atmospheric model forced by the observed SST simulates an internal heating term which is in poor agreement with the cloud convection data. The atmospheric model performs best when it is forced by a combination of observed SST and cloud convection data.

The failure of the ocean-atmosphere model to simulate the observed easterlies is not due to the atmospheric model component but to the oceanic one. Introducing altimetric zonal current anomalies in the SST equation improves the SST simulation by enhancing the contrast between cold and warm anomalies in the eastern Pacific, but not in the central Pacific. Adding air-sea flux in the SST equation improves the model performance because latent heat has a positive feedback on SST. In agreement with observations, it induces warm anomalies which are stronger and last longer than in the standard run. This improvement, however, takes place only in the central Pacific and latent heat helps to simulate cold anomalies in 1988 only west of the dateline. The cold anomaly, which was observed in 1988 in the central Pacific, is recovered only when the temperature of entrainment due to a thermocline upwelling is enhanced. This new parametrization of the temperature of entrainment is validated with the XBT temperature profiles.


## 1. Introduction

This paper is the second part of a study on El Niño-La Niña events over 1980-1993 using model simulations and various observations. The model is the one described in Zebiak and Cane (1987) and is named CZ model. Part 1 presents results on the comparison between observations and simulations obtained from a standard run of the CZ model in an uncoupled context: the ocean model is forced by FSU winds and the atmospheric wind is forced by the simulated SST. This run is named CR for "Control Run". This run provides initial conditions for the CZ model when it is run in a coupled mode for predictions.

Hoping that realistic initial conditions would increase the model skill in predicting the reality, we started our project with the coupled mode by assimilating altimetric data in the oceanic part of the CZ model, using a Kalman filtering technique as developed by Miller and Cane (1989). Indeed Fu et al (1993) have been quite successful in assimilating Geosat data with this latter approach. Recently, Fisher et al (1994) have been successful in improving the short-range forecasts of their coupled model by assimilating sea level observations in their ocean model. However, it turned out that assimilating data in the CZ model, even with optimal methods, was not worthwhile because the model did not have enough skill in simulating the reality.

Model data comparison in Part 1 has shown that most of all, the CZ model fails to reproduce the cold SST anomalies (Figure 1) and the easterly anomalies (Figure 2). It is not surprising then that the model performs very poorly in the coupled mode over this period. Thus it is worth examining the complex link between the atmospheric and the oceanic variables. To do so, we introduce data in the CZ model to force the various model components. The objective here is not to tune the model in order to minimize the

discrepancies but rather to understand why and how the model can be successful or not. In addition, because the CZ model is not designed to simulate the reality poleward of 10° of latitude, we concentrate only on the equatorial processes.

This paper is organized as follows. In section 2, we examine the atmospheric model response to various conditions prescribed for local heating and convection heating. In section 3, we examine the SST response to various conditions prescribed for zonal advection, air-sea fluxes and vertical entrainement. A summary and discussions are proposed in the last section.

## 2. The atmospheric model

Let us first examine the atmospheric model. Starting from a prescribed SST anomaly, the atmospheric model simulates a forcing which contains two terms. The main one corresponds to the local heating $Q_T$. It is a function of SST only. The second one $Q_C$ is a corrective term introduced to simulate the fact that the heating due to low-level moisture convergence anomaly is not dependant on SST only, but also on wind convergence. The two forcing terms (see Zebiak, 1986) can be written as:

$$Q_T = \alpha \, SST \times \exp\{(TBAR-30)/16.7\}$$

and

$$Q_C = \beta \, \{ M(cbar + c) - M(cbar) \}$$

where SST is the sea surface temperature anomaly, TBAR is the climatologic sea surface temperature, c and cbar are the anomalous and climatologic wind convergence and M is the function defined by:

$$M(x) = x \quad \text{if } x > 0$$

$$M(x) = 0 \quad \text{if } x < 0.$$

In the standard run, we have:

$\alpha = 0.03 \ m^2 s^{-3} (°C)^{-1}$ and

$\beta = 1.6 \times 10^4 \ m^2 s^{-2}$.

In the CZ model, the total forcing $Q_T+Q_C$ is an internal forcing which is supposed to represent the heating due to cloud convection. We examine below what the model response is in 4 cases. One corresponds to the forcing computed with observed SST (run A.SST), one to the same forcing but without the corrective term $Q_C$ (run A.SST0), one to the forcing computed with observed convection (run A.CVN0) and one to a forcing combining observed SST and observed convection (run A.SSTCVN).

### *2.1 Runs forced with observed SST anomalies: run A.SST and run A.SST0*

We first ran an experiment where the heating term $Q_T$ is prescribed with the AVHRR temperature anomalies instead of the simulated ones. Other than that, the model is run in its standard configuration: it computes its own correction $Q_C$ for moisture convergence by an iterative process, starting from the values at the previous time step only if NINO3(*) index is larger than 0.1°C. This run is named A.SST.

Zonal wind stress anomalies simulated in this run are presented along the equator in Figure 3. This wind is very different from the wind simulated in the CR and it is in pretty good agreement with the observations (compare Figure 3 with Figures 2). Run A.SST is able to reproduce the oscillations of the zonal wind pretty successfully over the whole period, with alternance of easterlies during cold events and westerlies during warm events. In particular, the anomalous easterlies are well recovered during La Niña in

1988. The agreement with the observed winds is significantly improved for both components along and outside the equator (see tables 1a and 1b). The amplitude of the wind anomalies is larger than in the CR. It is stronger than the observed one for the zonal wind, but it is in much better agreement with observations for the meridional wind. Correlations with observations are better for run A.SST than for the CR. Thus, the deficiency of the CZ model to simulate easterlies, is not due to the atmospheric component, but to the oceanic component. This is the most important message provided by run A.SST.

Besides this result, this run still presents some unrealistic features. We have seen in Part 1 that the CZ model simulates the strong zonal wind westerlies to the east of the observed ones and that the offset is particularly large for the wind stress curl anomalies both north and south of the equator. This is also the case for the run A.SST for both westerlies and easterlies (see Figure 4ab). The maxima of curl anomalies are located to the east of the observed one. The offset is not as dramatic as in the CR (compare with Figure 17ab in Part1), but it is still of the order of 20°. This is probably because the forcing term is not correctly simulated, even when it is computed with the observed SST anomalies.

The forcing term $Q_T+Q_C$ simulated in the run A.SST after the iterative process, is presented along the equator in Figure 5. It shows, as expected, that the atmosphere is losing heat during La Niña events in alternance with gaining heat during El Niño events. This was not the case for the CR and this is in much better agreement with the observed convection heating (the reader can refer to Part 1 to find the details in section 2 about the cloud convection data, in section 7 about the computation of the observed convection heating term and its comparison with the term

simulated in the CR). The forcing anomalies simulated in run A.SST have a larger amplitude than in the CR. This is also in better agreement with observations. However, the location of the simulated forcing anomalies still agree very poorly with the observed one. The simulated forcing is strong in the central and eastern Pacific, whereas for observations the strongest anomalies are located in the western Pacific between 150°E and 180°. This is because the CZ model simulates a forcing which is too tightly linked to the SST anomalies.

In order to examine the impact of the moisture convergence iterative process introduced in the model (Zebiak, 1982; 1986), we ran the model forced by SST without the corrective term $Q_C$. This run is named A.SST0. The wind simulated in run A.SST0 is close to the one simulated in run A.SST. $Q_C$ is a corrective term which is one order of magnitude smaller than $Q_T$. In addition, it has a spatial distribution very similar to $Q_T$. Results show that $Q_C$ tends to strengthen the equatorial wind anomalies (see tables 1a and 1b). This helps to confine the curl anomalies closer to the equator, as described in Zebiak (1985). However $Q_C$ does not help to simulate the wind anomalies further to the west. As in run A.SST, the wind curl simulated in run A.SST0 is badly located with a position to the east of the observed one (see Figure 4). Note that run A.SST performs less well than run A.SST0 in simulating the meridional wind component (see table 1b). As explained in Zebiak (1990), improvement is still needed to simulate the forcing due to cloud convection with a more realistic skill.

### *2.2 Runs forced with observed convection anomalies: run A.CVN0 and run A.SSTCVN*

We then ran an experiment, where at each time step and whatever the NINO3(*) SST value, the forcing is prescribed as:

$$Q_{obs} = \gamma \ CVCN,$$

where CVCN is the observed frequency of convection occurence in ($s^{-1}$) and $\gamma = 5.3 \times 10^4 \ m^2 \ s^{-2}$ (see Part 1). $Q_{obs}$ is introduced in the atmospheric model at each time step. The atmospheric model is then directly forced. In this run, there is no need for computing the wind convergence by iterative process as in the CR. This experiment is named A.CVN0.

Zonal wind stress anomalies simulated in run A.CVN0 are presented along the equator in Figure 6. In this run, the model is able to reproduce the strong easterlies in 1988 west of the dateline. Run A.CVN0 performs better than the CR for the meridional component over the central Pacific north and south of the equator (see table 1b). But the model simulates unrealistic zonal wind anomalies east of 160°W along the equator (see table 1a). Over NINO34(*), the zonal wind anomalies simulated in run A.CVN0 have indeed the wrong sign.

A plausible interpretation is that the heat released by cloud convection contributes to drive the surface winds in the western Pacific less than in the central and eastern Pacific because the heat is released over a thicker convective layer in the west. The heating has been prescribed in run A.CVN0 with a uniform $\gamma$. Indeed we were able to improve the simulations forced by the cloud convection data by weighting the forcing $Q_{obs}$ with a coefficient $\gamma$ increasing from west to east.

Another solution is to force the model with a combination of local and convection heating. We ran several experiments where the model was forced with both SST and cloud convection data. The run forced by observed SST

with $\alpha = 0.02\ m^2\ s^{-3}\ °C^{-1}$ and by observed cloud convection with $\gamma = 1.6 \times 10^4\ m^2\ s^{-2}$ is named Run A.SSTCVN. This choice of parameters $\alpha$ and $\gamma$ gives the smallest RMS difference with the observed zonal wind over NINO4(*). The zonal wind simulated in this run is presented in Figure 7. The agreement between the simulated and the observed zonal winds is quite good. It performs as well as the Run A.SST in terms of zonal wind (see Table 1a). It does much better for the meridional wind (see Table 1b). Run A.SSTCVN is the first run which is able to simulate the wind curl at the correct location (Figure 4ab). This is the case both south and north of the equator. This is a major improvement compared to the runs A.SST or A.SST0.

All these results indicate that reality is more complex than what can be simulated with the atmospheric model used in CZ. In a baroclinic model, as assumed in (Gill, 1980; Zebiak, 1982; 1986), the forcing is an internal one assumed to represent the organized convection. Run A.SST0 shows that the parametrization of convection heating in terms of SST does not simulate a realistic forcing. Run A.SST shows that little is improved when the parametrization is also a function of surface wind convergence. Run A.CVN0 shows that a realistic internal heating does not allow the recovery of realistic surface winds. A model based on a boundary layer forced by SST anomalies only (see Lindzen and Nigam (1987)) would not do better. Neelin (1989) has shown that the boundary layer model is equivalent to Gill(1980)'s model. Both models have oversimplified physics which do not allow the representation of the vertical shear between the surface and the altitude where the cloud convection heat is released. One solution is to use a more sophisticated atmospheric model. Another one is to revisit the

parametrization of moisture convergence proposed in CZ. A satisfactory theory giving the relationship between cloud convection, SST and wind convergence is still lacking (Neelin and Held, 1987). We are currently investigating a parametrization depending on the climatologic cloud convection rather than the climatologic wind convergence. Indeed these two climatologic fields are quite different. First the term defined as a function of wind convergence with the M function as in CZ is highly non linear. This means that the climatology computed with a linear approximation, M(cbar), is very different from the climatology which we computed by taking the 12 monthly averages of M(cbar+c) over 1980-1993. This is evidenced along the equator in Figures 8ab. Secondly, those two fields have their stronger amplitude in the central and eastern Pacific whereas the observed climatologic convection field is the strongest in the central and western Pacific (Figure 8c). Thus a forcing term parameterized as a function of climatologic cloud convection instead of wind convergence should contribute to generate wind anomalies further to the west of the SST anomalies.

Nevertheless, the reader should not forget the main result of this section. The CZ model performs much better in simulating wind when the atmospheric component is forced with observed SST. In this case, the model recovers the easterlies which are missing in the CR. This strengthens the need for improving the SST simulations.

## 3. The surface layer model

Let us examine the simulations of SST by the ocean component of the CZ model. We have seen in Part 1 section 5, that the CR is missing the cold SST anomalies in the Central Pacific in 1988. We examine here how

those can be recovered, by changing the zonal advection (run O.U1), adding air-sea fluxes (run O.LHSR), or changing the vertical upwelling (run $O.T_{sub}$).

### *3.1 Zonal advection : run O.U1*

As found by various authors (e.g, Gill, 1983; Harrison and Schopf, 1983; Latif et al, 1988; Zebiak, 1985; McPhaden and Picaut, 1990; Cane et al, 1990), the role of zonal advection in the SST changes is dominant over NINO4(*). In the CZ model (as in Battisti and Hirst, 1989), the nonlinearity of the model is taken into account by a development to the first order in current anomaly. Thus the zonal advection contains two terms:

$$- \quad U0 \quad x \quad (TBAR + T)_x \qquad (1)$$

$$- \quad UBAR \quad x \quad (T)_x \qquad (2)$$

where U0 and UBAR are the anomalous and climatologic zonal currents, T and TBAR are the anomalous and climatologic SST. We have seen in Part 1 that term (1) is the dominant term for observations and that it is oscillating at a 9-month frequency for simulations. The 9-month oscillations, due to the resonant mode of the basin, can be reduced by increasing the friction, but then, the energy at low-frequency is overly damped compared with observations. Eliminating the wave reflection is not a realistic solution either (see run O.BNDY0 in Part 1).

Alternatively, we can examine the role of anomalous zonal advection by inserting the altimetric currents in the CZ model. The friction and the boundary conditions are the standard ones as in the CR. At each time-step, the baroclinic zonal current derived from Geosat (see Part 1) is introduced in the surface layer model to compute the term (1) of the SST equation. This run is named O.U1. The SST simulated in this run is presented along the

equator in Figure 9a. It can be compared with the CR or the observations (Figure 1).

Compared to the CR, the cooling in 1988-1989 is enhanced in the far eastern Pacific. The SST simulated in run O.U1 (as in run O.BNDY0 and as in observations) has a tendancy to propagate westward at O(90 cm/s) in 1988. This speed corresponds to the phase speed of the first meridional Rossby wave for the first baroclonic mode. This is an example where the dominant mechanism involved to determine SST is the zonal advection and not the thermocline displacement (which would give an eastward migration along the equator). However, the model still fails to reproduce the cold anomaly in 1988 in the central Pacific. The agreement with the observations is not better than for the CR (see table 2). This supports the idea that the model deficiency in simulating cold anomalies does not come from inadequate simulation of the zonal anomalous current.

Forced by the SST simulated in run O.U1, the atmospheric model simulates easterlies which migrate from the eastern to the western Pacific in 1988 (Figure 9b). This is also found in observations and not in the wind simulated in the CR. However the apparition of these easterlies is quite brief. The model is still missing most of the wind anomaly sitting in the central Pacific in 1988.

### *3.2 Weights of the terms in the SST equation*

It is *a priori* surprising that although the zonal advection governs most of the SST tendancy, changing the zonal advection as in Run O.U1 does not have a strong impact on the simulated SST over NINO4(*). We examine here the weights of the various terms involved in the SST equation. This equation (see Zebiak and Cane, 1987) can be written as:

$$
\begin{array}{llcll}
\partial T/\partial t = & - \; U0 & \times & (TBAR + T)_x & (1) \\
& - \; UBAR & \times & (T)_x & (2) \\
& - \; V0 & \times & (TBAR + T)_y & (3) \\
& - \; VBAR & \times & (T)_y & (4) \\
& - \; \{M(WT)-M(WBAR)\} & \times & TBAR_z & (5) \\
& - \; M(WT) & \times & (T-Te) / H1 & (6) \\
& - \; \alpha_s & \times & T & (7)
\end{array}
$$

where: $M(x) = x$ if $x > 0$,

$M(x) = 0$ if $x < 0$.

Terms (1) and (3) correspond to the advection by the anomalous currents U0 and V0 of the temperature (climatology TBAR + anomaly T). Terms (2) and (4) correspond to the advection by the climatologic currents UBAR and VBAR of the temperature anomaly T. Terms (5) and (6) correspond to the vertical advection and depend on the sign and magnitude of the vertical velocity. Term (5) corresponds to the advection by the anomalous current of climatologic temperature. It is a function of the total upward velocity M(WT) and the climatologic upwelling M(WBAR). Term (6) is the climatologic upwelling M(WBAR) of anomalous temperature. The anomalous vertical gradient of temperature is defined as the difference between the sea surface temperature anomaly T and the entrainment temperature $T_e$. $T_e$ is parameterized as a function of the climatologic and the anomalous thermocline depth. Term (7) is a damping term. In the standard run, $\alpha_s$=(125 days)$^{-1}$.

The relative weight of these terms vary with longitude and latitude. Away from the equator, the meridional advection term (4), plays a strong role. Meridional transport of heat associated with El Niño-La Niña

oscillations has been previously studied by various authors (e.g. Zebiak, 1989; Miller and Cheney, 1990; Philander and Hurlin, 1988). Here, we rather concentrate along the equator where the meridional advection terms are negligible. We have seen that the zonal advection (term (1)+term (2)) explains most of the SST changes over NINO4(*). Along the equator, this is the case for the simulations in the CR (Figure 10a) and to a large extent for observations (Figure 10b). But this does not mean that the other terms are negligible. Along the equator, the upwelling terms and the damping term have similar amplitude to zonal advection. For the CR (Figure 10c), it is striking that the two upwelling terms (terms (5) and (6)) have opposite signs and are cancelling each other. For observations (Figure 10d), it is striking that the anomalous advection of mean temperature (term 5) and the damping term (term 7) have opposite signs and are cancelling each other. We then examine if those terms are adequately simulated. The SST in the CZ model is not forced by air-sea fluxes. The damping term introduced for numerical reasons, is not likely to adequately represent these fluxes. Let us first examine the role of latent heat and solar radiation.

### *3.3 Heat flux: run O.LHSR$_{obs}$ and run O.LHSR*

In this section, we examine the impact of adding air-sea fluxes in the SST equation. To the first approximation, when studying the thermal forcing of the ocean over interannual time scales, the changes in sensible heat and long-wave radiation can be neglected compared to the changes in latent heat and solar radiation. Seager et al (1988) have shown that adding latent heat and solar radiation fluxes in the CZ model significantly improves the simulation of climatologic SST. Seager (1989) pointed out that the cloud

cover reduces the solar heating during the El Niño 1982/1983 and 1986/1987 events, but that it has a moderate influence on the SST simulations. Here, we reexamine these questions for both warm and cold events. We also examine the impact of latent heat.

Because latent heat is a coupled process between the atmoshpere and the ocean, we ran two sorts of experiments where we added heat flux in the SST equation. One is a prescribed forcing which is applied using the data sets of solar radiation and latent heat anomalies that we were given. This experiment is named O.LHSR$_{obs}$ and these fluxes are named "observed" fluxes. The second one consists of computing the solar radiation and the latent heat flux from the model outputs with the objective of coupling the ocean-atmosphere in the future. For the present time, the model is not run in a coupled system. This second experiment is named O.LHSR and these fluxes are named "parameterized" fluxes. Even in an uncoupled context, these two experiments can be quite different because the wind can drive oceanic currents which can induce an SST anomaly inconsistent with the prescribed thermal forcing. In this case, run O.LHSR would simulate a latent heat which is different from the prescribed one. Another reason for running these two experiments is their duration. In the prescribed case, the extent of the experiment is limited to the period between July 1987 and December 1990 covered by the latent heat data set (see Part 1). This is a short period of time and run O.LHSR$_{obs}$ starts from strongly anomalous conditions. In the second case, the solar radiation is parameterized as a function of cloud convection and the latent heat is parameterized as a function of simulated SST and wind speed. Details about the various parametrizations used are given in the appendices 1 and 2. Because the simulated cloud convection simulated by the CR is deficient, we used the model output for the latent heat

only. We used the cloud convection data for computing the parameterized solar radiation. Thus results for run O.LHSR cover the period from July 1983 to December 1990. Parameterized latent heat flux computed with various bulk formula, SST and wind speed are presented in Appendix 2. The parameterized estimates presented here correspond to the Formula (2) in Appendix 2 applied on the wind simulated in run A.SST. Our objective here being a qualitative description of the role of air-sea flux on the model simulations, we present the common features found in all experiments and describe which errors the model can simulate because of uncertainties in the estimation of latent heat.

Anomalies of solar radiation are mostly located over the central and western equatorial Pacific and along the ITCZ and the SPCZ. They correspond to less heat gained by the ocean during El Niño (as clouds inhibit radiation) and more heat during La Niña. The amplitude of the change in heating is of the order of 100 $W/m^2$ over the central Pacific along the equator. The corresponding forcing term is $\lambda \times 0.94$, where $\lambda = (\rho\ Cp\ H1)^{-1} = 4.10^{-3}\ J\ K^{-1}m^{-1}$ where $\rho$ is the water density, Cp is the heat capacity of water and H1 is the surface layer thickness equal to 50m. Results averaged over NINO4eq are plotted in Figure 10e. The forcing term due to solar radiation is as strong as the upwelling term (5) in the SST equation. Solar radiation works as a damping term. It is larger than the damping simulated in the CR in the central and western Pacific. It is smaller in the east. Moreover solar radiation damps less during La Niña periods than during El Niño periods.

Anomalies of latent heat are mostly located over the central equatorial Pacific and along the ITCZ and SPCZ. Over the central equatorial Pacific, the agreement between the observed and the parametrized latent heat is good

regardless of the parametrization used (see Appendix 2). Evaporation is reduced during El Niño 1987 and increased during La Niña 1988. This corresponds to a variation of 200W/m$^2$ in latent heat over the central Pacific along the equator. The forcing term due to latent heat, $\lambda \times Q_{LH}$, is larger than any of the terms studied above (Figure 10e). In addition, its sign is so that latent heat has a positive feedback on SST. During El Niño, although SST is warmer than usual, less evaporation takes place and the ocean gains heat because the wind speed is reduced. During La Niña, although the ocean is cooler than normal, evaporation increases and it tends to cool the ocean because the trade winds are stronger than usual. This is so because latent heat is much more sensitive to wind than to SST (see Appendix 2).

Overall, the net heat flux due to solar radiation and latent heat is the strongest in the central Pacific whereas the damping assumed in the CZ model is the strongest over NINO3(*). It corresponds to a heat gain during El Niño and a heat loss during La Niña, with the loss stronger than the gain. Thus, adding the air-sea fluxes in the SST equation may help recover the cold SST anomalies which are missing in 1988 in the CR.

Experiments where we added air-sea fluxes consist in adding the net flux ($0.94\ \lambda\ Q_{SR} - \lambda\ Q_{LH}$) in the SST equation, everything else being the same as in the CR. For the second experiment O.LHSR, several runs were performed depending on the wind (FSU or simulated winds) or on the formula (see Appendix 2). Results are presented for the formula (2) applied on the wind simulated in run A.SST as above. Note that because the parameterized latent heat is not much sensitive to SST, the latent heat computed with the SST simulated in the run O.LHSR or in the CR is very

similar to the one computed with the observed SST, even in 1988 when the SST simulated in the CR agrees so poorly with the observed SST.

The SST simulated along the equator is presented in Figure 11a for the run O.LHSR$_{obs}$ and Figure 11b for the run O.LHSR. We find some similar characteristics in both runs. Along the equator, in the western Pacific, both runs simulate cold anomalies at the end of 1983-beginning of 1984 and at the end of 1988-beginning of 1989. These are not simulated in the CR. These are found in the observations. During the ending phase of El Niño 1987, the SST anomaly in the central Pacific is warmer by 1°C than in the CR. This is also in closer agreement with the observations. However adding heat flux does not allow the model to simulate a cold SST anomaly in the central Pacific in 1988. In addition, it does not improve the SST simulations east of 120°W along the equator. This is where the parameterized latent heat is the most uncertain (see Appendix 2).

The wind anomalies simulated by run O.LHSR$_{obs}$ or run O.LHSR are strongly affected (Figure 12a and 12b). They do not always agree better with the observed wind anomalies than the winds simulated in the CR. In the western Pacific, the cold anomalies recovered in both runs in 1988 allow simulation of the easterlies as observed. The stronger warm anomalies in 1987 also allow simulation of stronger westerlies as observed. Indeed these runs perform well in simulating the zonal wind anomalies west of the dateline. But both runs perform poorly east of 160°W. Strong westerlies are simulated in the central Pacific in 1988 and 1989. Easterlies are simulated east of the westerlies during El Niño 1987. These are quite strong for the run O.LHSR. None of those are present in the observed winds. The two wind components simulated in run O.LHSR agree poorly with observations over NINO4 (see Table 1a and 1b). This is because wind is sensitive to the SST

gradient and adding air-sea fluxes have improved the SST in the western/central Pacific, but not east of 160°E. The performance of run O.LHSR in simulating the wind is the worst because the parameterized latent heat is uncertain in the eastern Pacific. During the period August-December 1987 (Figure 13ab), run O.LHSR simulates a warm SST anomaly which is maximum at 160°W. So it simulates easterlies on the western side of the SST anomaly and westerlies on its eastern side. Similarly, over August-December 1988 (Figure 13cd), run O.LHSR simulates a minimum SST anomaly at 160°E and a maximum SST anomaly at 120°W. So this run simulates converging winds towards the warm anomaly and diverging ones away from the cold anomaly.

In summary, adding latent heat and solar radiation in the SST equation has a strong impact on the SST and wind simulations. For all experiments, it improves the model perfomance in simulating the SST and wind west of the dateline. It does not improve the SST in the eastern Pacific nor the wind east of the dateline. In addition the parameterized latent heat contains errors in the eastern Pacific. The major source of error is due to the assumption that the relative humidity is a constant field in time and space. This implies that the parameterized latent heat is not sensitive to SST and that the simulations forced by a prescribed latent heat are not very different when the latent heat is adjustable as in reality. Nevertheless uncertainties in the heat flux parametrization cannot account for the model failure to simulate the cold SST in the central Pacific in 1988. A similar conclusion is proposed in Seager and Blumenthal (1994) for the simulation of the climatologic SST using the CZ model. We have seen that zonal advection is not either responsible for the model deficiency. Let us now concentrate on the vertical upwelling.

### *3.4 Vertical upwelling: run O.$T_{sub}$*

Over NINO4(*), the model simulates a vertical advection by mean upwelling of anomalous temperature (term (6)) which tends to cool down the SST during El Niño events and to warm it up during La Niña events (Figure 10c). The anomalous temperature gradient in term (6) is computed from the difference between the SST and the temperature at the bottom of the surface layer $T_{sub}$. The model simulates a $T_{sub}$ which is anomalous during El Niño periods only. The simulated $T_{sub}$ can be compared with the temperature anomalies at 50m observed with XBT. These have a negative peak in the central Pacific in 1988 which is as strong as the positive peak in 1987. Indeed when computed with observed SST and observed $T_{sub}$, term (6) is very weak (see Figure 10d).

In the control run, $T_{sub}$ is parameterized as a function of the mean and anomalous thermocline depth, respectively hbar and h, and has the form:

$$T_{sub} = T1 \{ \tanh [ b1 (hbar+h) ] - \tanh [ b1 \ hbar ] \} \quad \text{if } h > 0 \quad \text{(downwelling)},$$

or

$$T_{sub} = T2 \{ \tanh [ b2 (hbar-h) ] - \tanh [ b2 \ hbar ] \} \quad \text{if } h < 0 \quad \text{(upwelling)}.$$

The mean thermocline hbar is a function of longitude provided in the code. Values of the four parameters T1, T 2, b1 and b2 are:

$$T1 = 29°C \quad \text{and} \quad b1 = (80m)^{-1}$$

$$-T2 = 40°C \quad \text{and} \quad b2 = (33m)^{-1}.$$

The $T_{sub}$ anomalies simulated in the CR are plotted as a function of the simulated thermocline anomalies at six various locations along the equator (Figure 14). This figure shows that $T_{sub}$ is assumed much more sensitive to

| | | | |
|---|---|---|---|
| T1 | = | +30°C | West of 130°W |
| b1 | = | $(110\ m)^{-1}$ | " " " " " " " " " " " " " " " " " " |

T1 and b1 increase linearly up to 40°C and $(33m)^{-1}$ between 130°W and 100°W.

and everywhere, we have: T2 = -T1 and b2 = b1

This means that:

1) $T_{sub}$ variations are symmetric for downwelling and upwelling: this confirms that the impact of upwelling on SST is overly restricted in the standard run.

2) $T_{sub}$ is less sensitive to thermocline changes in the eastern Pacific than what is assumed in the standard model.

We then ran the model with these new parameters. This run is named O.$T_{sub}$. The SST simulated in this run is presented along the equator in Figure 15a. The new formulation of $T_{sub}$ is very helpful in recovering the cool event in 1988 (see table 2). Forced with these SST anomalies, the atmospheric model also performs well: it simulates the strengthening of the easterlies in 1988 (Figure 15b, table 1a). Compared to the CR, the simulations of the meridional component is slightly improved, but it is still poor (table 1b). We then introduced a climatologic thermocline depth hbar with a meridional structure as described in Appendix 3. This run, named O.$T_{suby}$, does not improve the simulation of the meridional wind component either (table 1b). This is because the effet of the mean upwelling is very confined to the equator.

### *3.5 Combined forcing: O.LHSR$_{obs}$T$_{sub}$ and O.LHSRT$_{sub}$*

Lastly, we ran experiments with this new parametrization and with adding the air-sea heat fluxes as in the Run O.LHSR$_{obs}$ and O.LHSR. Other than this, everything else is set to the standard configuration as in the CR. These runs are named O.LHSRT$_{sub}$ and O.LHSR$_{obs}$T$_{sub}$. The objective is to examine the role of the air-sea fluxes in a model where the vertical mixing is more realistically parameterized. We concentrate on the cold events because results for the warm events are the same as for the runs O.LHSR$_{obs}$ and O.LHSR.

Adding heat flux contributes to strengthen the cold anomaly in 1988 (Figure 16a). The agreement with observed SST over NINO4 is the best among all the runs (Table 2). But the SST in the western Pacific is then colder than the observed one. This explains why run O.LHSR$_{obs}$T$_{sub}$ simulates a strong westerly in the western Pacific and a strong easterly in the eastern Pacific. Therefore the simulated wind anomalies are stronger than what is observed or simulated in the run O.T$_{sub}$ (Figure 16b). This happens because wind is very sensitive to small changes in SST gradients. Thus adding air-sea fluxes in the run O.T$_{sub}$ has degraded the simulations of the zonal wind (table 1a). This is also the case for the meridional component (table 1b). It is not likely that the errors in the parametrized flux are responsible for this degradation because run O.LHSR$_{obs}$T$_{sub}$ is also less performant than O.T$_{sub}$ in 1988-1989. It is possible that improving the forcing conditions for the SST equation does not improve the SST because the model does not have the adequate physics to respond to this forcing. In reality, thermodynamic forcing like wind generates some oceanic circulation.

## 4. Summary and perspectives

In this paper, a variety of *in situ* and satellite observations are used to prescribe the forcing in the CZ model over 1980-1993. The reader must remember that we concentrate our effort in the equatorial band only, knowing that the CZ model is not designed to simulate off-equatorial processes. Our objective was to recover the cold anomalies in the central and eastern Pacific and the strengthening of the easterlies in the central Pacific which the model fails to simulate in 1988-1989 when it is run in an uncoupled context with its standard parametrization.

The CZ model can be corrected for this deficiency by changing the parametrization of the temperature of entrainment so that its cooling due to a thermocline shoaling be as strong as its warming due to a thermocline deepening. This new parametrization is validated with the XBT data. Running the model with this new parametrization improves the agreement with observations because the mean upwelling of anomalous temperature no longer has a dampening role. With this new parametrization, both the SST and the wind anomalies are improved. Note that results with this new parametrization have been presented in an uncoupled context. Results in a coupled context are quite different.

Because all the errors in simulating the wind, the ocean dynamics and the SST get accumulated in a coupled context, we have further examined how the simulations in the uncoupled mode could become more realistic by prescribing various forcing conditions. The runs presented in this paper lead to the following conclusions.

* When the atmospheric model is forced by observed convection anomalies, it is able to simulate wind anomalies at the correct location if the forcing is applied with a weight increasing from west to east. When the atmospheric model is forced by observed SST anomalies, it is able to

simulate wind anomalies at the correct location if the forcing is applied with a weight increasing from east to west. These two results are consistent with the fact that neither SST by itself nor convection by itself can simulate correctly the surface wind because the atmospheric layer is actually vertically sheared. The best simulations of winds are obtained when the model is forced by a combination of local heating and cloud convection.

* When altimetric observations are used to prescribe the baroclinic zonal current anomalies in the SST equation, the model simulates stronger SST anomalies in the eastern Pacific and the westward propagation of anomalies is enhanced.

* Latent heat estimated with various bulk formula based on wind speed and SST has been intercompared with independant observations. Although the estimates present large uncertainties, common features were identified. Latent heat fluctuates by O(200W/m$^2$) between events. This is is twice larger than the flux anomalies due to solar radiation. Latent heat has a positive feedback on SST anomalies. Solar radiation has a damping role which is stronger in the central and western Pacific than in the eastern Pacific, and also larger during El Niño events than during La Niña events. Adding the net heat flux in the CZ model increases the intensity and duration of the SST anomalies in the central and western Pacific. Errors in the latent heat can have a negative impact on the SST simulations in the eastern Pacific and therefore can degrade the wind simulations in the central Pacific.

* It is certainly worth taking all these modifications into account for improving the SST and the wind simulations. This means that the baroclinic model must be refined. One possibility which is in current investigation is to add a second baroclinic mode. Results also indicate that the forcing of the atmospheric model must be revisited. One possibility which is under current

investigation is to parameterize the forcing with a term dependant on the climatologic cloud convection and not on the climatologic wind convergence, as those two quantities are proportional. Lastly, it is worth introducing latent heat and solar radiation because they play a dominant role in the SST and wind changes. Because of missing information about the relative humidity fields, the parametrization of latent heat used in this study is based on the assumption that these fields are constant in space and time. This leaves a small role to the ocean in generating the amount of heat which is exchanged with the atmosphere. In reality latent heat is a fully coupled ocean-atmosphere process, and for the ocean, the heat flux is a function of SST, the simulated SST evolution should be different from the one in response to a prescribed latent heat flux. In addition, introducing heat flux in the SST equation which does not influence the ocean dynamic as in the CZ model is not realistic either. The ocean model does not have the physics to correctly account for the heat flux at the surface. This could also imply that another ocean model is needed. Actually, with more sophisticated models, the uncertainty of the air-sea fluxes is also a major difficulty in simulating the SST in the tropical Pacific ocean (Stockdale, 1993).

Overall, the main result of this paper is that the model is mostly sensitive the vertical advection. Vertical mixing is indeed one of the most difficult term to simulate. This is also the case for more sophisticated models (Philander et al, 1992). The parametrization of the vertical mixing in those models is still under investigation and changing the turbulence closure scheme has a strong impact on simulations (see e.g. Blanke and Delecluse, 1993). The approach chosen in the CZ model is a heavy parametrization with an empirical formula containing four parameters. We surely do not want to recommand the values proposed in this paper as definitive. It will be worth

determining a new parametrization with an optimal method of assimilation where both oceanic and atmospheric variables are assimilated once the model has been improved with the various modifications proposed above. It will also be worth examining the impact of these modifications in a coupled context.

**(*) Endnote:**

Regions designed with (*) in the text, figure or table captions correspond to:

NINO3: (5°S-5°N, 90°W-150°W),

NINO34: (5°S-5°N, 120°W-180°),

NINO4: (5°S-5°N, 150°W-160°E),

NINO4N: (1°N-7°N, 150°W-160°E),

NINO34N: (1°N-7°N, 120°W-180°),

NINO4S: (1°S-7°S, 150°W-160°E),

NINO34S: (1°S-7°S, 120°W-180°),

NINO4eq: (1°S-1°N, 150°W-160°E).

**ACKNOWLEGMENTS**

Most of all, the authors thank Dr S. Zebiak (LDEO, Palisades) who provided the code and data files. They thank him for his fruitful advice on the problems with the atmospheric model. They thank Dr. T. Liu (from JPL, Pasadena) for providing the heat flux and solar radiative budgets and the Liu and Niiler (1990) code to compute latent heat. They thank Dr. R. Seager (LDEO, Palisades) for providing information about the computation of latent

heat flux. They thank Dr. W. White and Dr. S. Pazan (from SCRIPPS, La Jolla) for the XBT data. This paper benefited from Dr S. Zebiak's and Dr. M. Cane's comments. They also thank Ken Clarke (USC, Los Angeles) for editing the manuscript in English.

The research described in this paper was carried out by the authors at the Jet Propulsion Laboratory, California Institute of Technology, under contract with the National Aeronautics and Space Administration.

# APPENDIX 1

## Parametrization of solar radiation

Solar radiation is a function of seasonal earth inclination and cloud cover. The anomalous radiation is proportional to the anomalous cloud cover. One can use the anomalous cloud convection heating as a measure of the cloud cover. This allows to compute the anomalous solar radiation from the model outputs only. However, as long as the CZ model is not improved for simulating this heating, we cannot use the simulated cloud convection. We used the data of anomalous cloud convection and converted them from frequency into fraction of cloud cover by a linear regression.

As in Weare et al (1981), we chose the parametrization defined in Reed (1977). It is suggested by Simpson and Paulson (1979) to be in best agreement with observations. The solar radiation Qc can be computed as follows:

$$Qc = Qo(1 - \alpha)(1 - AC + 0.0019\beta)$$

where:

$\alpha$ = 0.06 is the albedo,

A = 0.62 is a constant,

C is the fractional cloud cover,

$\beta$ is the noon solar attitude in degrees,

Qo is the solar radiation under clear skies following Seckel (1970):

$$Qo = (A_0 + A_1\cos\Phi + B_1\sin\Phi + A_2\cos 2\Phi + B_2\sin 2\Phi).$$

where $\Phi$ is $2\pi/[365(t - 21)]$, t being the Julian day,

$A_i$ and $B_i$ are latitude-dependent coefficients given by Reed (1977).

The observed and parameterized solar radiation are compared along the equator in Figure A1.1. The agreement is good in timing, amplitude and location. It is very good over NINO4 (see Figure 10e in the text). It was checked that the agreement is good outside the equator as well (see table A1). The parameterized and observed heats have very similar spatial patterns. The parameterized heat has a stronger amplitude outside the equatorial central Pacific. Using the same parametrization, errors of the same order were found by Seager and Blumenthal (1994) when comparing the climatologic solar radiation derived from the data provided by the International Satellite Cloud Climate Project (ISCCP) with the one derived from the Earth Radiation Budget Experiment (ERBE).

## APPENDIX 2

### Parametrization of latent heat

The generally accepted method of computing heat flux is based on a bulk formula. If the wind speed |v| is larger than a minimum value Vmin for the evaporation to take place, latent heat flux is computed as:

$$LH = \rho_a C_E L |v| [qs - qd] \quad (1)$$

where:

$\rho_a = 1.2 \times 10^{-3}$ g cm$^{-3}$ is the air density,

$L = 2.501 \times 10^6$ J kg$^{-1}$ is the latent heat of vaporization,

$C_E$ is the turbulent exchange coefficient,

|v| is the wind speed,

qs is the saturation specific humidity at the sea surface temperature T,

qd is the saturation specific humidity at the dew point temperature $T_d$.

A common approximation consists in assuming that the relative humidity r = qd/qa is a constant. Although this approximation can be responsible for errors above 50W/m2 (Liu and Niiler, 1990), we followed this approach because the relative humidity is not provided by the model. Following Seager et al (1988), we checked that assuming an air temperature parallelling the SST is equivalent to assuming that the saturation specific humidity of the atmosphere qa is proportional to the saturation humidity of the ocean qs. So finally, the latent heat that we computed is derived from the formula:

$$LH = \rho_a C_E L |v| (1-\delta) qs(T) \quad (2)$$

where $C_E = 1.3 \times 10^{-3}$ and $\delta = 0.8$ as in Blumenthal and Cane (1989) and the saturation specific humidity qs is evaluated from the Clausius-Clapeyron equation (see Bolton, 1980).

Latent heat anomalies computed with (2) were found sensitive to the values of wind, to the parameter Vmin and to the way the climatology and anomaly are determined. In order to do so, we computed the total latent heat, using the total wind $V_{TOT}$, the climatologic wind $V_{BAR}$ and the anomalous wind V0. Two methods were tested to compute the latent heat anomalies Q0. The first one consists in writing the following 4 options:

if $|V_{TOT}| > Vmin$ and $|V_{BAR}| > Vmin$, $Q0=LH(V_{TOT}) - LH(V_{BAR})$

if $|V_{TOT}| > Vmin$ and $|V_{BAR}| < Vmin$, $Q0=LH(V_{TOT})$

if $|V_{TOT}| < Vmin$ and $|V_{BAR}| > Vmin$, $Q0= - LH(V_{BAR})$

if $|V_{TOT}| < Vmin$ and $|V_{BAR}| < Vmin$, $Q0=0$

This corresponds to the approach chosen by Zebiak and Cane (1987) for computing the convection term in the atmospheric model or the upwelling term in the SST equation. This approach is valid in a linear context. The second method consists of computing the total latent heat, computing its climatology and subtracting it from the total to derive the anomaly.

The observed latent heat is presented along the equator in Figure A2.1. Figures A2.2 to Figures A2.5 correspond to some of the various estimates we tested. All of them were computed with formula (2) with the AVHRR SST anomalies or the SST simulated in the CR and the climatologic SST field used in the CZ model. Figure A2.2 corresponds to the latent heat anomaly computed with the wind anomalies simulated in run A.SST, with the climatologic wind field used in the CZ model, assuming a Vmin of 4.8 m/s and computing the anomaly with the 4 options. Observed and parameterized anomalies have similar characteristics in terms of amplitude and timing (see Figure 10e in the main text). However, differences

with the observed latent heat can reach locally 50 $W/m^2$. The largest differences are located in the eastern Pacific. In the central and western Pacific, the parameterized anomalies do not have a correct location and do not extend as much in longitude. In the eastern Pacific and outside the equator, the amplitude of the paramerized latent heat is stronger than the observed one (see table A2). Nevertheless, among the various ones tested, this is the estimate which agrees the best over NINO4 with the observations. This is the parameterization which is used in run O.LHSR and run $O.LHSRT_{sub}$.

Figure A2.3 corresponds to the same estimate, except for the value of Vmin which is set to 4m/s. Then the increase of evaporation in 1988 is even more confined to the western Pacific.

Figure A2.4 corresponds to the estimate computed as in Figure A2.2, except for the wind fields which are the FSU anomalous and climatologic fields. Then, the latent heat is stronger than 100 $W/m^2$ during 2 years in 1988 and 1989 which is unrealistic. In addition, it has a strong climatologic signal showing up in the eastern Pacific. So we determined the latent heat anomalies by computing the climatologic latent heat over 1982-1991 (Figure A2.5). This makes a difference which can be larger than 50 $W/m^2$ at several times and various locations, especially in the eastern Pacific.

Lastly we applied Liu and Niiler (1990)'s formula to the AVHRR SST and the FSU wind. This formula corresponds to formula (1) with a coefficient $C_E$ depending on the stability of the atmosphere. Because we did not have estimates of qd, we applied (1) with a relative humidity equal to 0.7 and the saturation specific humidity computed with the temperature of the air Ta = SST - 0.5. The anomaly was computed without

making the linear approximation. Then, for all the cases of SST and winds we tested, the estimated latent heat anomalies are a lot weaker than the observed ones (Figure A2.6). The difference can be as large as the order of $50W/m^2$ when assuming a constant relative humidity of 80% like in the previous cases. The latent heat data set we have was computed with the Liu and Niiler's formula as here, but with a relative humidity derived from the SSMI data. This means that it is necessary to have the relative humidity fields to adequately estimate the latent heat using the Liu and Niiler's formula.

So this appendix suggests that the latent heat is highly dependent on the formula used, mostly because of the variations of the relative humidity. When this quantity is not known and assumed constant in space and time, using formula (2) provides latent heat flux with errors which can reach 100 W/m2. This assumption implies that latent heat is not sensitive to SST. In 1988, although the temperature anomaly simulated by the CR is warmer by 2°C than the observations, formula (2) used with the simulated SST agrees within less than $15W/m^2$ with the estimate computed with the observed SST. Thus this assumption leaves a small role to the ocean in generating the amount of heat exchanged via evaporation and this is far from reality.

With formula (2), latent heat mostly responds to wind changes. Estimates are sensitive to the threshold Vmin and to the way the anomaly is computed within $50W/m^2$. Errors are the largest in the eastern Pacific.

# APPENDIX 3

## Climatologic thermocline depth

The thermocline depth $hbar_{CZ}$ used in the parametrization of $T_{sub}$ in the standard version of the code is a function of longitude only (Figure A3.1). We used the Levitus (1982) data set to determine a thermocline depth as a function of longitude, latitude and time in order to examine the sentivity of the parametrization $T_{sub}$ to hbar. We computed the surface dynamic height relative to 2000dbar, using the monthly temperature fields and annual mean salinity fields provided by Levitus (1982). We then subtracted to this field a constant value equal to the spatial averaged value of the yearly mean height along the equator. We then converted this relative quantity into thermocline depth using a commonly adopted density ratio ($3*10^{-3}$). We then added a mean constant of 110m. We call this estimate of thermocline $hbar_{LEV}$. It is a function of longitude, latitude and time.

$hbar_{LEV}$ is plotted along the equator in Figure A3.1 for the months of April and October and for its yearly averaged value. $hbar_{LEV}$ can differ from $hbar_{CZ}$ by O(50m). We used the yearly averaged values of $hbar_{LEV}$ to determine the optimal parametrization of $T_{sub}$ along the equator with the XBT anomalies as described in section 3.4.

Then, we ran several experiements to examine the sensitivity of the CZ model to the values of hbar. Run $O.T_{sub}$ presented in section 3.4 corresponds to the new parametrization of $T_{sub}$ with the yearly averaged values of $hbar_{LEV}$ along the equator only. We then ran an experiment where the yearly averaged values were replaced by the monthly values. This had little impact on the simulations. We then ran an experiment where $hbar_{LEV}$ is the yearly averaged field as a function of longitude and latitude. This run

corresponds to run $T_{suby}$ in section 3.4. The averaged meridional structure between the dateline and 140°W is plotted relative to the equator in Figure A3.2. This also has little impact on the simulations.

## References

Battisti, D.S. and A.C. Hirst, 1989: Interannual variability in a tropical atmosphere-ocean model: influence of the basic state, ocean geometry and nonlinearity. *J. Atmos. Sci.*, **46**, 1687-1712.

Blanke B. and P. Delecluse, 1993: Variability of the tropical Atlantic Ocean Simulated by a general Circulation Model with Two Different Mixed Layer Physics, J. Phys. Oceanog., **23**, 1363-1388.

Blumenthal, B. and M.A. Cane, 1989: Accounting for parameter uncertainties in model verification: an illustration with tropical sea surface temperature. *J. Phys. Oceanog.*, **19**, n°6, 815-830.

Bolton, D., 1980: The computation of equivalent temperature, *Mon. Wea. Rev.*, **108**, 1046-1053.

Cane, M. A., 1992: Comments on "the fast-wave limit and interannual oscillations". *J. Atmos. Sci.*, **20**, 1947-1949.

Fisher M., M. Latif, M. Flugel and J. Zhou, 1994: Assimilation of Sea Level Data into a Primitive Equation Model of the tropical Pacific, *TOGA Notes*, **15**, 1-5.

Fu L.L., I. Fukumori and R.N. Miller, 1993: Fitting dynamic models to the Geosat sea level observations in the tropical Pacific Ocean. Part 2: a linear wind-driven model, *J. Phys. Oceanog.*, **23**, 2162-2182.

Gill, A. E., 1980: Some simple solutions for heat induced tropical circulation. *Q. J. R. Meteor. Soc.*, **106**, 447-462.

Gill, A. E., 1983 : An estimation of sea level and surface current anomalies during the 1972 El Niño and consequent thermal effects. *J. Phys. Oceanog.*, **13**, 586-607.

Harrison, D. E. and P.S. Schopf, 1984: Kelvin wave induced anomalous advection and the onset of surface warming on El Niño event. *Mon. Wea. Rev.*, **112**, 923-933.

Latif, M., A. Sterl, E. Maier-Reimer, and M. M. Junge, 1993: Climate variability in a coupled GCM. Part I: The tropical Pacific. *J. Climate*, **6**, 5-21.

Levitus S., 1982: Climatological Atlas of the world ocean, *NOAA professional Paper* 13, US Dept of Commerce, Rockville, MD 174pp.

Lindzen, R.S. and S. Nigam, 1987: On the role of sea surface temperature gradients in forcing the low-level winds and convergence in the tropics. *J. Atmos. Sci.*, **45**, 2440-2458.

Liu, W. T., K. B. Katsaros and J. A. Businger, 1979: Bulk parametrization of air-sea exchanges of heat and water vapor including the molecular constraints at the interface. *J. Atmos. Sci.*, **36**, 1722-1735.

McPhaden, M., and J. Picaut, 1990: El Niño-Southern Oscillation displacements of the western Equatorial Pacific warm pool. *Science*, **250**, 1385-1388.

Miller R.N. and M.A. Cane, 1989: A Kalman Filter Analysis of sea level height in the tropical Pacific Ocean, *J. Phys. Oceanog.*, **19**, 773-790.

Miller L. and R.E. Cheney, 1990: Large-scale Meridional Transport in the tropical Pacific Ocean during the 1986-1987 El Niño From Geosat, *J. Geophys. Res.*, **95**, 17905-17919.

Neelin, J. D., 1989: On the interpretation of the Gill model. *J. Atmos. Sc.*, **46**, 2466-2468.

Neelin, J. D. and I. M. Held, 1987: Modeling tropical convergence based on the moist static energy budget. *Mon. Wea. Rev.*, **115**, 3-12.

Philander, S. G. H. and W.J. Hurlin, 1988: The heat budget of the tropical Pacific Ocean in a simulation of the 1982-1983 El Niño. *J. Phys. Oceanog.*, **18**, 926-931.

Philander, S. G. H., R. C. Pacanovski, N-C. Lau, and M. J. Nath, 1992: Simulation of ENSO with a global atmospheric GCM coupled to a high-resolution tropical Pacific Ocean GCM. *J. Climate*, **5**, 308-329.

Reed, R. K., 1977: On estimating insolation over the ocean. *J. Phys. Oceanog.*, **7**, 482-485.

Rosati, A. and K. Miyakoda, 1988: A general circulation model for upper ocean simulation. *J. Phys. Oceanog.*, **18**, 1601-1626.

Seager, R., S. Zebiak and M. A. Cane 1988: A model of the tropical Pacific Sea surface temperature Climatology. *J. Geophys. Res.*, **93**, 1265-1280.

Seager R., 1989: Modeling Tropical Sea Surface Temperature: 1970-1987. *J. Phys Oceanog.*, **19**, 419-431.

Seager R. and M.B. Blumenthal, 1994: Modeling tropical Pacific sea surface temperature with satellite-derived solar radiative forcing, submitted to *J. Climate*.

Seckel, G. R., 1970: The trade wind zone oceanography pilot study Part VIII: Sea-level meteorological properties and heat exchange processes July 1963 to June 1965. *Report-Fisheries* , N° 612, 129 pp.

Simpson, J. J. and C. A. Paulson, 1979: Mid-ocean observations of atmosphere radiation. *Quart. J. Roy. Meteor. Soc.*, **105**, 487-502.

Stockdale T., D. Anderson, M. Davey, P. Delecluse, A. Kattenberg, Y. Kitamura, M. Latif, T. Yamagata, 1993: "Intercomparison of tropical Ocean GCMs", Report from the TOGA-NEG, WCRP-79, WMO/TD n°545, Case Postale 2300, CH-1211 Geneva, 20, Switzerland, 63 pp.

Weare, B. C., P. T. Strub and M. D. Samuel, 1981: Annual mean surface heat fluxes in the tropical Pacific ocean. *J. Phys. Oceanog.*, **11**, 705-717.

Zebiak, S.E., 1982: A simple atmospheric model of relevance to EL Niño, *J. Atmos. Sci.*, **39**, 2017-2027.

Zebiak, S. E., 1985: Tropical Atmosphere-Ocean Interaction and the El Niño-Southern Oscillation phenomenon. *PhD theses* at MIT, 261 pp.

Zebiak, S. E., 1986: Atmospheric convergence feedback in a simple model for El Niño. *Mon. Wea. Rev.,* **114**, 1263-1271.

Zebiak, S. E., and M.A. Cane, 1987: A model El Niño-Southern Oscillation. *Mon. Wea. Rev.*, **115**, 2262-2278.

Zebiak, S. E., 1989: Oceanic heat content variations and El Niño cycles. *J. Phys. Oceanog.*, 475-486.

Zebiak, S. E., 1990: Diagnostic studies of Pacific Surface winds. *J. Climate*, **3**, 1016-1031.

**Figure Caption**

Figure 1: SST as a function of longitude along the equator and time between January 1980 and April 1993. Results correspond to the CR (left) or to AVHRR observations (right). Units are °C.

Figure 2: Zonal stress as a function of longitude along the equator and time between January 1980 and April 1993. Results correspond to the CR (left) or to the FSU observations (right). Units are dyn/cm$^2$.

Figure 3: Zonal stress as a function of longitude along the equator and time between January 1982 and August 1991. Results correspond to run A.SST. Units are dyn/cm$^2$.

Figure 4: Variability of the curl over 1982-1991 as a function of longitude. Plots are averaged in the 3$^o$N-9$^o$N band (a) and averaged in the 3°S-9°S band(b). Units are $10^{-7}$ Pa/m.

Figure 5: Atmospheric forcing term as a function of longitude along the equator and time. Results correspond to run A.SST between January 1982 and August 1991 (left) or to observations between July 1983 and December 1990 (right). Anomalies are positive when the atmosphere is losing heat. Units are (50 m$^2$s$^{-3}$).

Figure 6: Zonal stress as a function of longitude along the equator and time between July 1983 and December 1990. Results correspond to run A.CVN0. Units are Dyn/cm$^2$.

Figure 7: Same as Figure 6 for run A.SSTCVN.

Figure 8: Climatologic convection as a function of longitude along the equator and month from January to December. Figure 8a corresponds to the parametrization M(cbar), where cbar is the climatologic wind convergence provided in the code. Figure 8b corresponds to the climatologic quantity [M(c)]bar, which is determined from the total field

M(c) computed with the convergence c of the total FSU wind over the period January 1980-April 1994. Figure 8c corresponds to the observed climatologic cloud convection. Units are $10^{-6}$ $s^{-1}$.

Figure 9a: SST as a function of longitude along the equator and time between April 1985 to September 1989. Results correspond to run O.U1. Units are °C.

Figure 9b: Zonal wind as a function of longitude along the equator and time between April 1985 to September 1989. Results correspond to run O.U1. Units are Dyn/$cm^2$.

Figure 10: Time evolution of the terms governing the SST equation. Terms have been averaged over 150°W-160°E along the equator. Signs are positive when the ocean gains heat. Units are °C $(month)^{-1}$. For Figures 10a and 10c, results are derived from the CR. For Figures 10b and 10d, results are derived from the observations: AVHRR for SST anomalies, altimetric currents for anomalous currents and climatologic fields of temperature and currents provided by Zebiak. For Figure 10d, Tsub is the temperature at 50m derived from XBT observations (See Section 3.4). Figure 10e corresponds to the forcing term due to solar radiation or latent heat with thick line for observed fluxes and thin lines for parameterized fluxes.

Figure 11: SST as a function of longitude along the equator and time. Results corresponds to run $O.LHSR_{obs}$ between July 1987 and December 1990 (a) or to run O.LHSR from July 1983 to August 1991 (b). Units are °C.

Figure 12: Zonal wind stress as a function of longitude along the equator and time. Results corresponds to run $O.LHSR_{obs}$ (a) between July 1987

and December 1990 or to run O.LHSR (b) between July1983 and August 1991. Units are Dyn/cm$^2$.

Figure 13: SST and zonal wind anomaly as a function of longitude along the equator. Plots have been averaged for the periods August to December 1987 or August to December 1988.

Figure 14: Temperature at 50m as a function of thermocline depth anomaly at 160°E, 180°E, 200°E, 225°E, 250°E, and 270°E. Plain line corresponds to the parameterization used in the control run, "+" to the XBT observations and dashed line to the curve which best fits the XBT data.

Figure 15a: SST as a function of longitude along the equator and time between February 1980 and April 1993. Results corresponds to run O.$T_{sub}$. Units are °C.

Figure 15b: Zonal wind stress as a function of longitude along the equator and time between February 1980 and April 1993. Results corresponds to run O.$T_{sub}$. Units are Dyn/cm$^2$.

Figure 16: SST (a) and zonal wind (b) anomaly as a function of longitude along the equator. Plots have been averaged over August to December 1988.

Figure A1.1: Solar radiation as a function of longitude along the equator and time from July 1983 to August 1991 for observations (a) and for the parametrization described in the Appendix 1 (b). Units are $W/m^2$.

Figure A2.1: Latent heat anomalies as a function of longitude along the equator and time from July 1987 to December 1990. Units are $W/m^2$. The plot corresponds to the observed anomalies.

Figure A2.2: Same as Figure A2.1 for the parameterized latent heat between January 1982 and December 1991. Results are derived using formula (2) with Vmin = 4.8 m/s, the wind anomaly simulated in run A.SST, the wind climatology used in the CZ model. The anomalies were computed using linear approximation.

Figure A2.3: Same as Figure A2.2 except for Vmin = 4 m/s.

Figure A2.4: Same as Figure A2.2 except for the wind anomalies and climatology which correspond to the FSU winds.

Figure A2.5: Same as Figure A2.4, except that the computation of anomalies has not been linearized.

Figure A2.6: Same as Figure A2.5, but computed with Liu and Niiler's formula.

Figure A3.1: Climatologic thermocline depth as a function of longitude along the equator. Plain line corresponds to $hbar_{LEV}$ and dashed or dotted lines to $hbar_{LEV}$ for the month of April, October and the yearly mean.

Figure A3.2: Yearly mean thermocline depth $hbar_{LEV}$ averaged over 140°W-180° as a function of latitude. The plot is relative to the mean value at the equator.

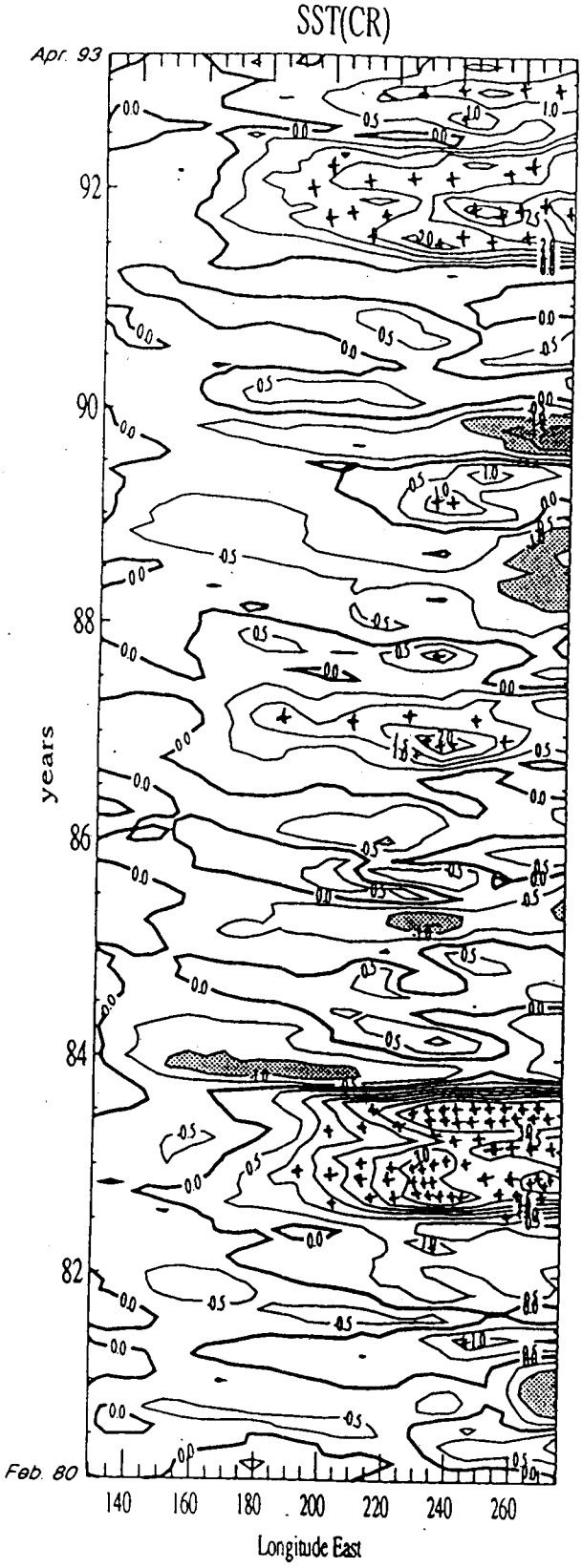
SST(CR)
Apr. 93
Feb. 80
years
92
90
88
86
84
82
140
160
180
200
220
240
260
Longitude East

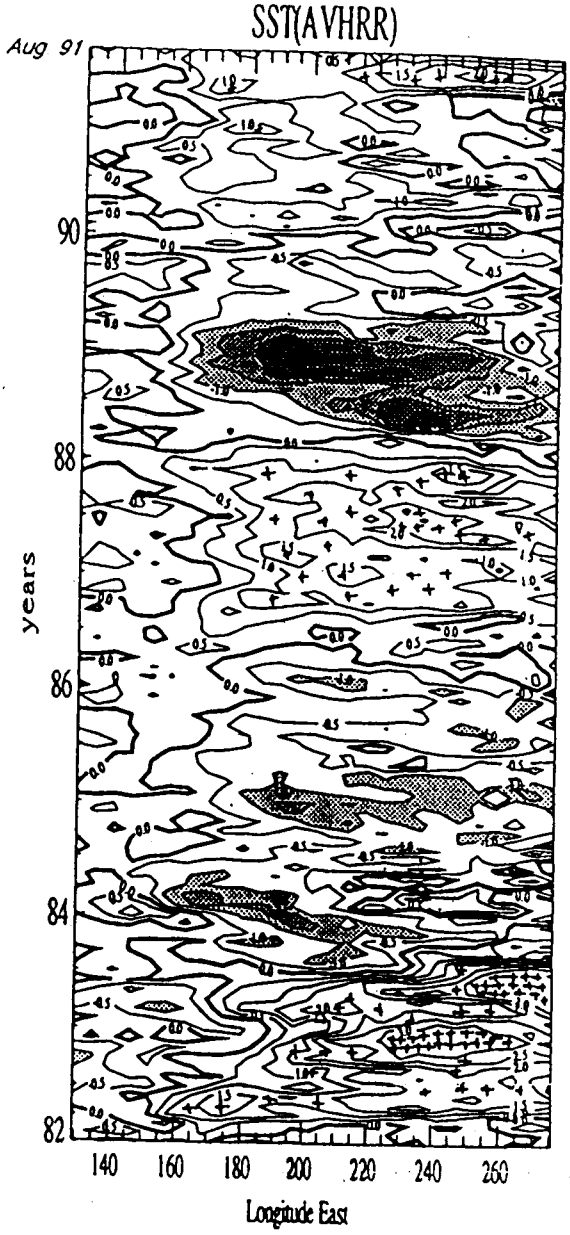
SST(AVHRR)
Aug 91
years
90
88
86
84
82
140
160
180
200
220
240
260
Longitude East

Fig. 1ab

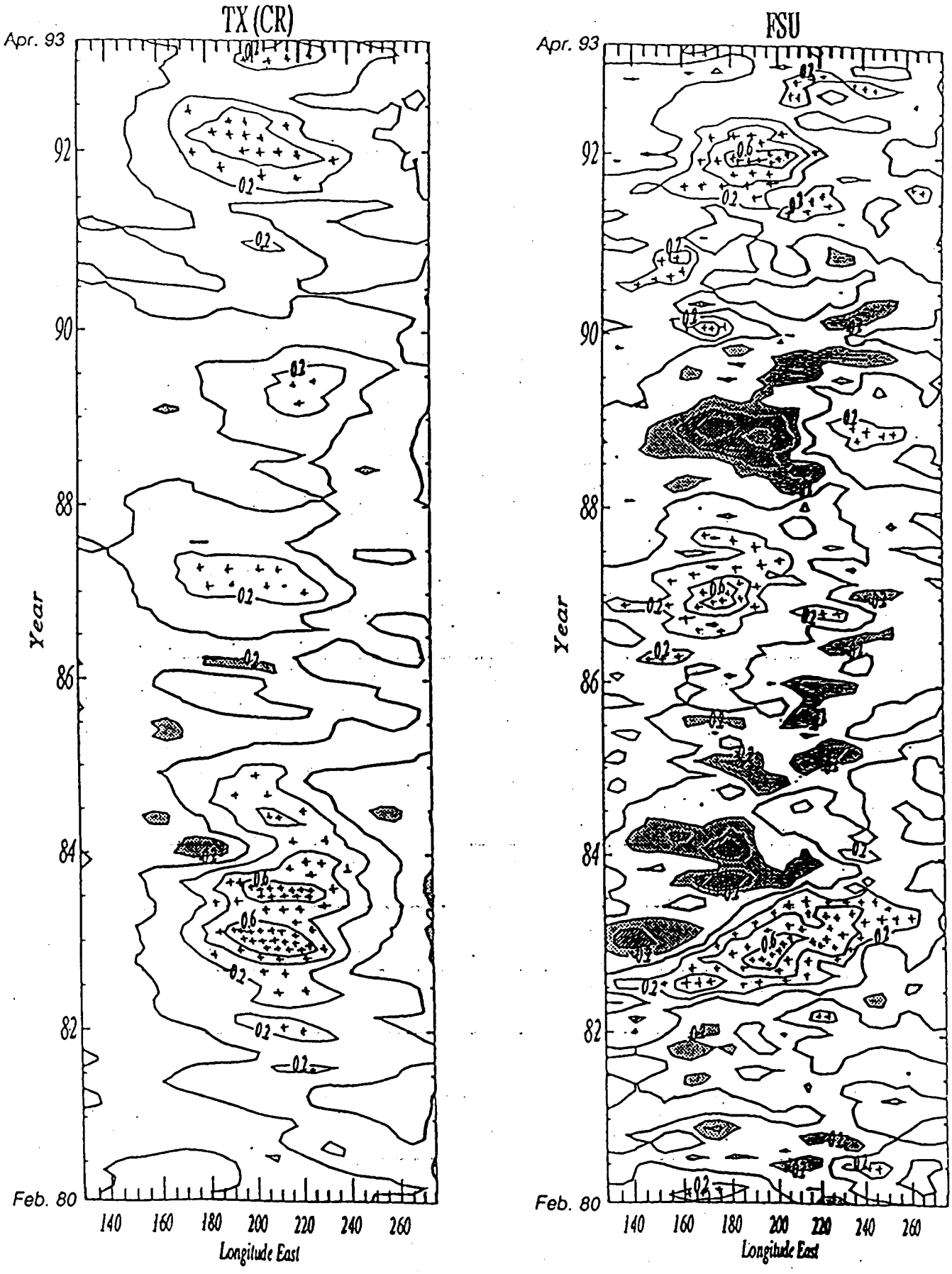
TX (CR)
FSU
Apr. 93
Feb. 80
Year
92
90
88
86
84
82
140
160
180
200
220
240
260
Longitude East

Fig. 2ab

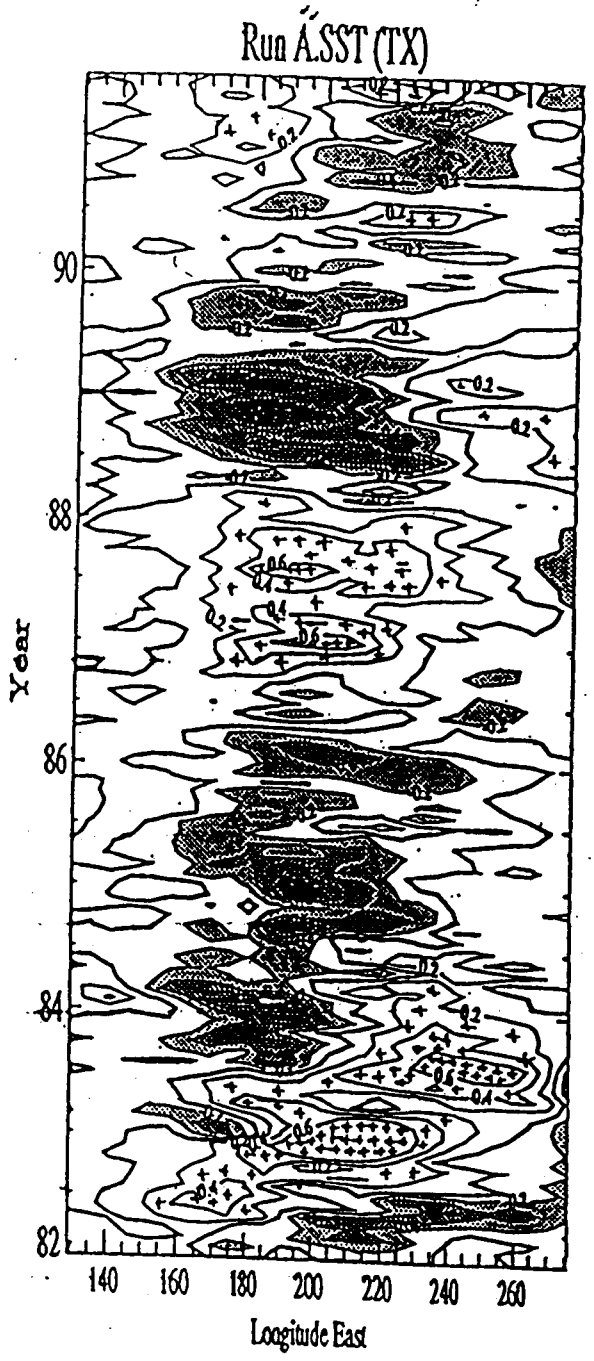
Run Á.SST (TX)
90
88
86
84
82
Year
140
160
180
200
220
240
260
Longitude East

Fig. 3

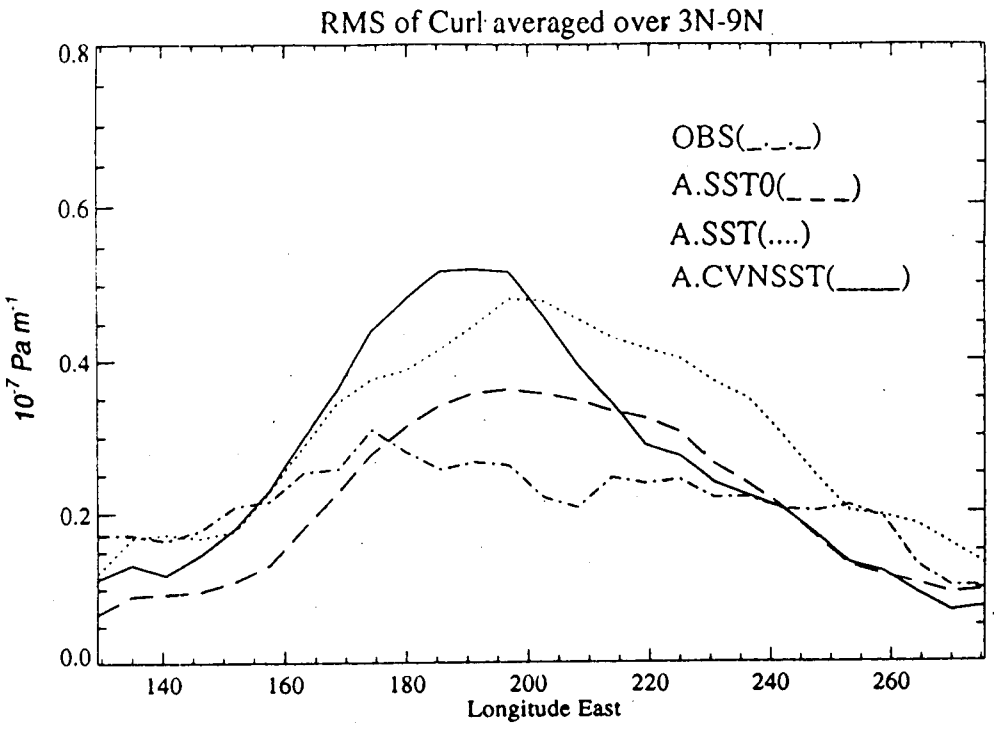
RMS of Curl averaged over 3N-9N
OBS(_._._)
A.SST0(_ _ _)
A.SST(....)
A.CVNSST(____)
$10^{-7}$ Pa m$^{-1}$
0.0
0.2
0.4
0.6
0.8
140
160
180
200
220
240
260
Longitude East

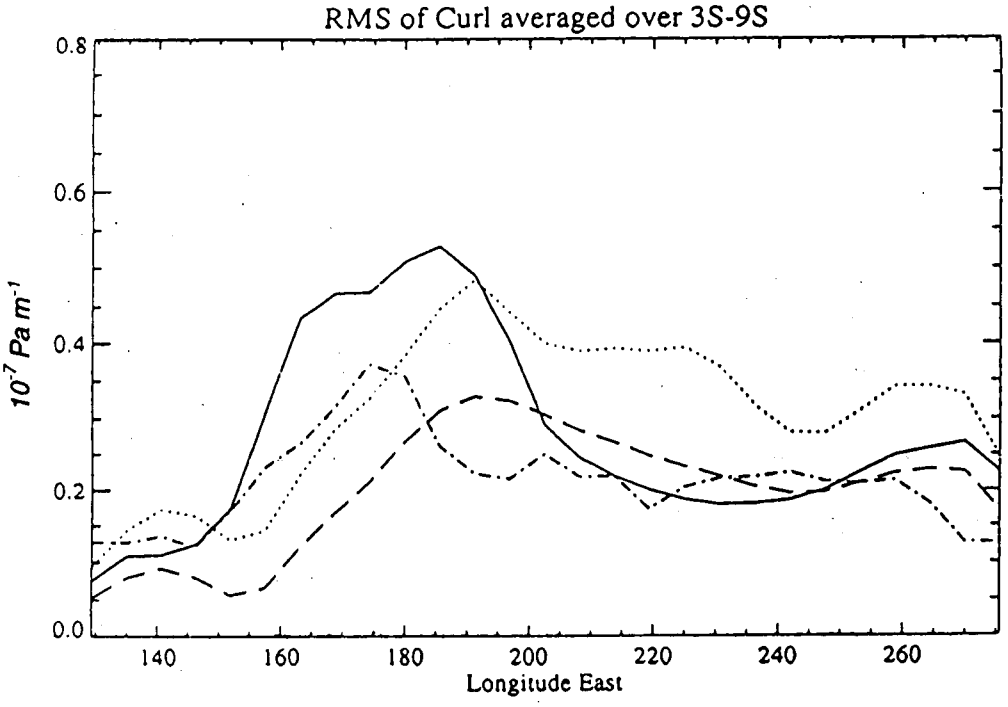
RMS of Curl averaged over 3S-9S
$10^{-7}$ Pa m$^{-1}$
0.0
0.2
0.4
0.6
0.8
140
160
180
200
220
240
260
Longitude East

4ab

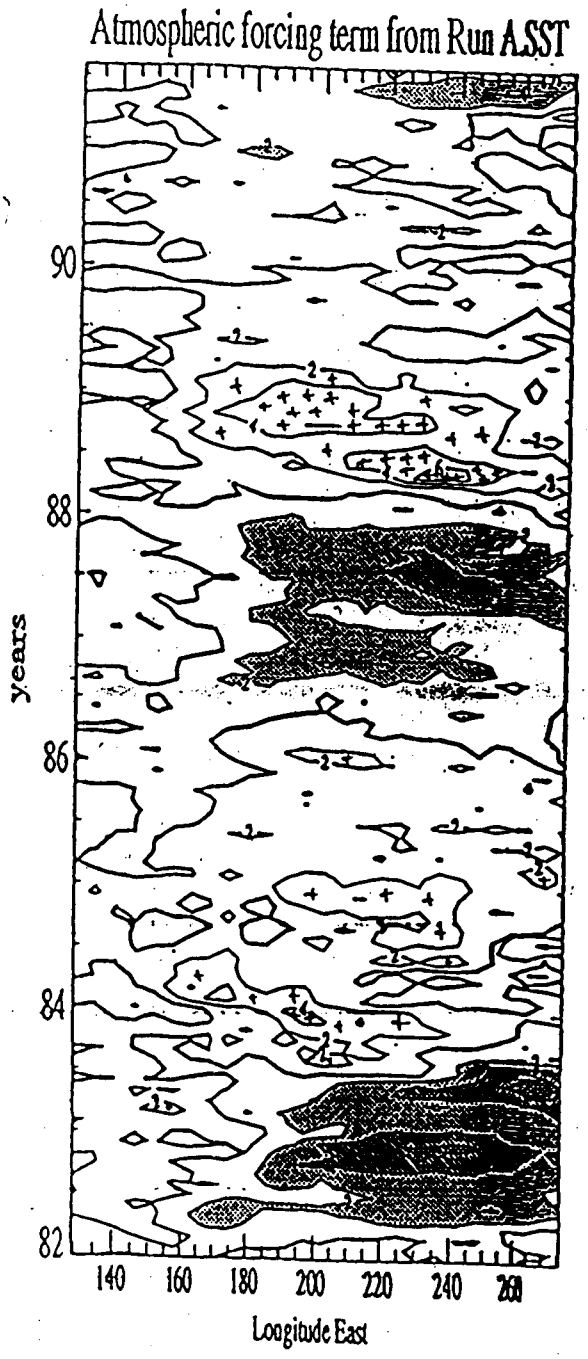
Atmospheric forcing term from Run A.SST
years
90
88
86
84
82
140
160
180
200
220
240
260
Longitude East

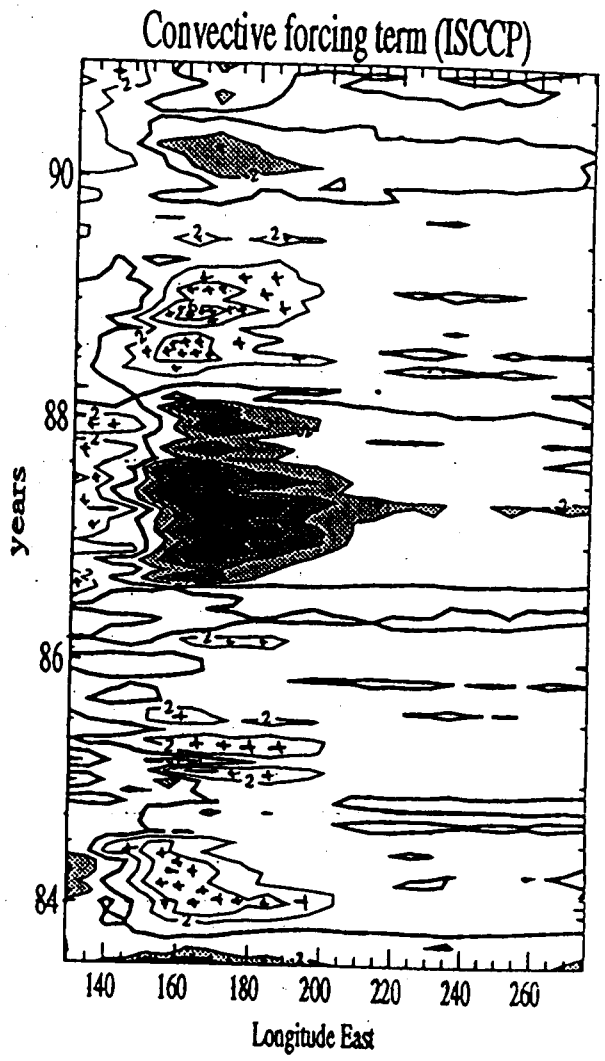
Convective forcing term (ISCCP)
years
90
88
86
84
140
160
180
200
220
240
260
Longitude East

Fig. 5

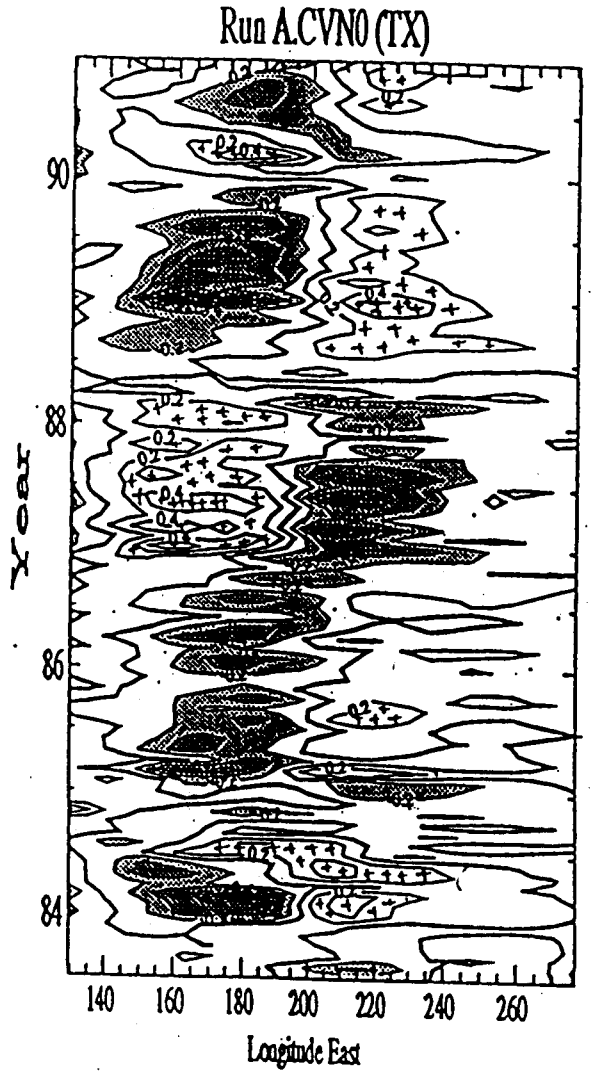
Run A.CVN0 (TX)
90
88
86
84
Year
140
160
180
200
220
240
260
Longitude East

Fig. 6

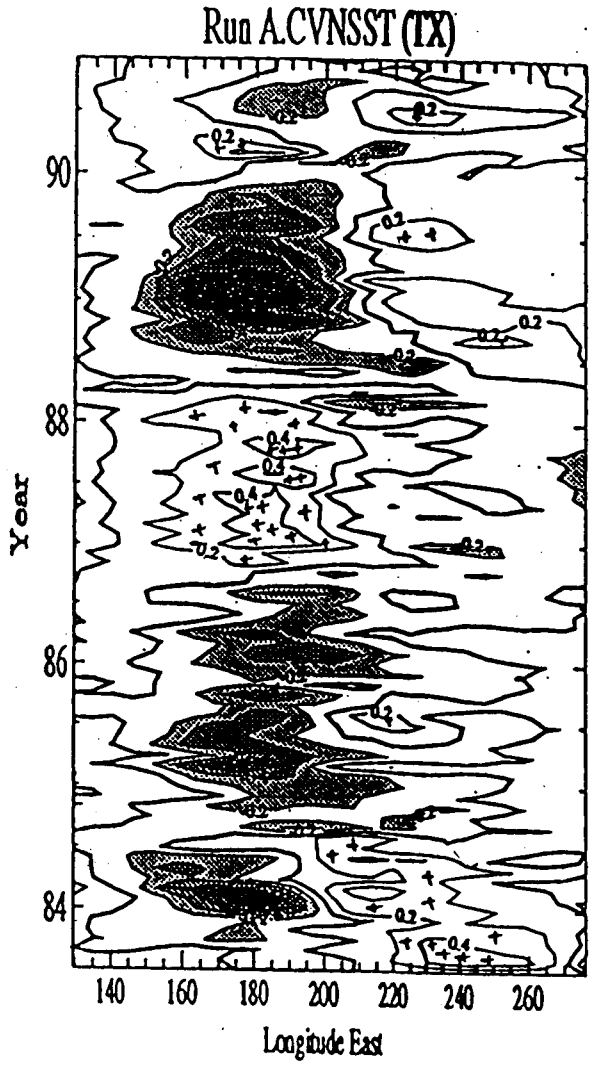
Run A.CVNSST (TX)
Year
90
88
86
84
140
160
180
200
220
240
260
Longitude East

Fig 7

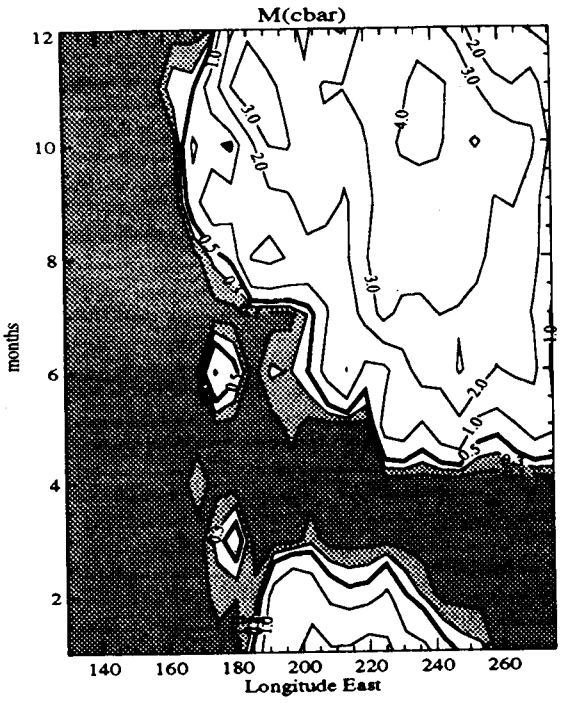
M(cbar)
months
Longitude East

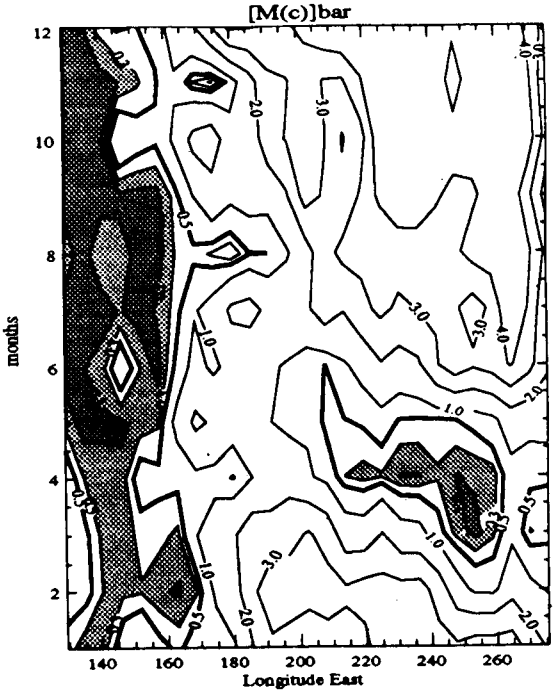
[M(c)]bar
months
Longitude East

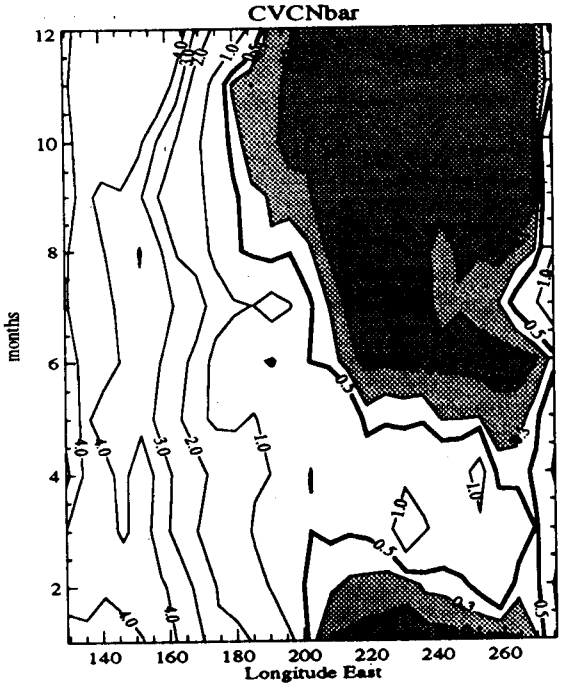
CVCNbar
months
Longitude East

Fig. 8abc

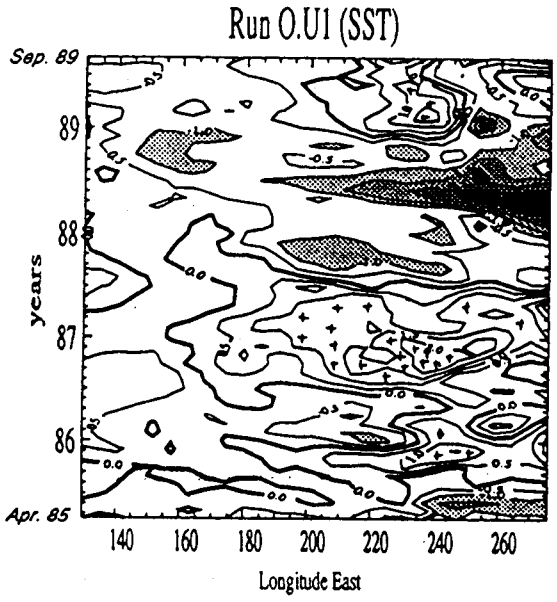
Run O.U1 (SST)
Sep. 89
Apr. 85
years
89
88
87
86
140
160
180
200
220
240
260
Longitude East

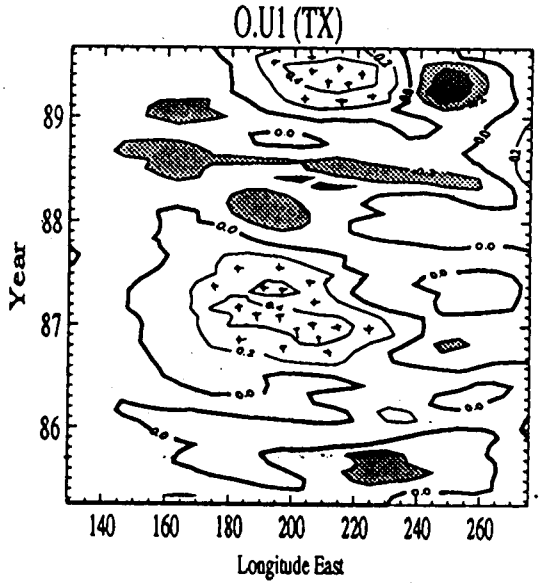
O.U1 (TX)
Year
89
88
87
86
140
160
180
200
220
240
260
Longitude East

Fig. 9ab

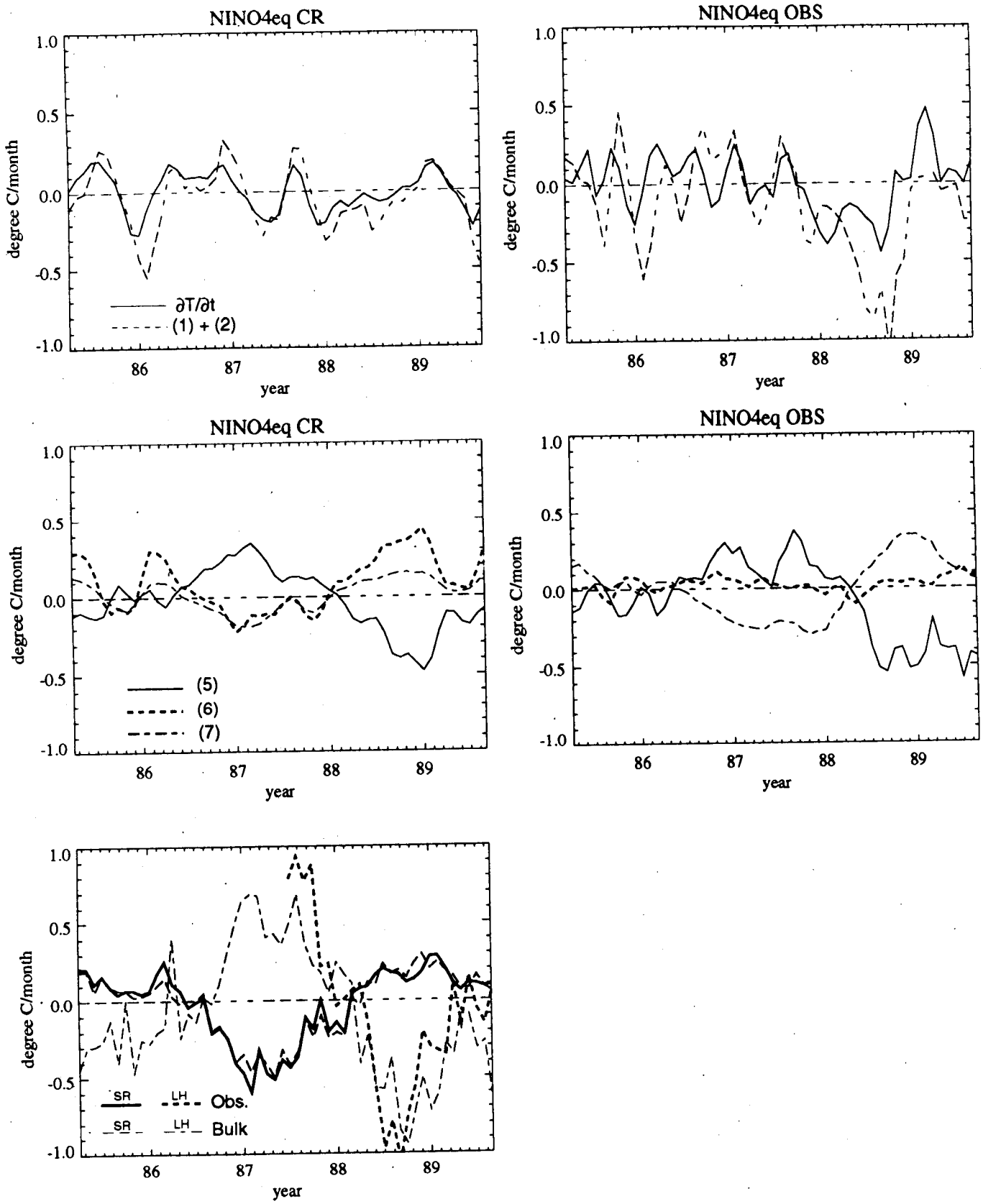
NINO4eq CR
NINO4eq OBS
degree C/month
year
∂T/∂t
(1) + (2)
(5)
(6)
(7)
SR
LH
Obs.
Bulk
1.0
0.5
0.0
-0.5
-1.0
86
87
88
89

Fig. 10abcde

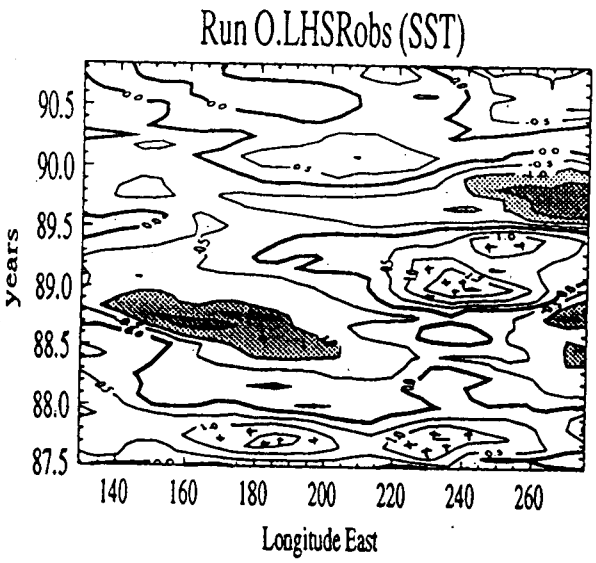
Run O.LHSRobs (SST)
years
90.5
90.0
89.5
89.0
88.5
88.0
87.5
140
160
180
200
220
240
260
Longitude East

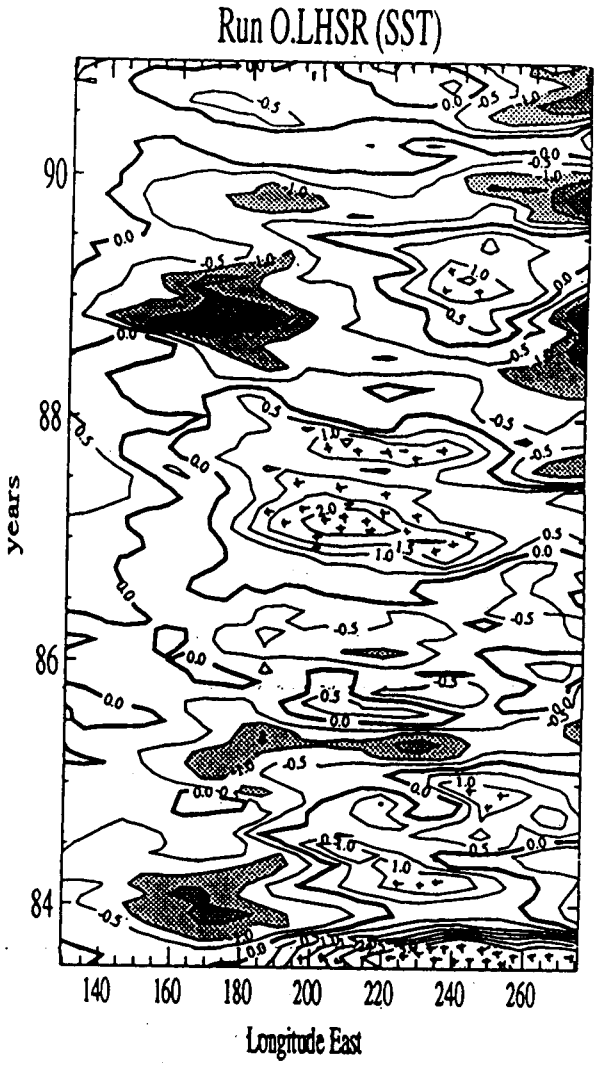
Run O.LHSR (SST)
years
90
88
86
84
140
160
180
200
220
240
260
Longitude East

Fig. 11ab

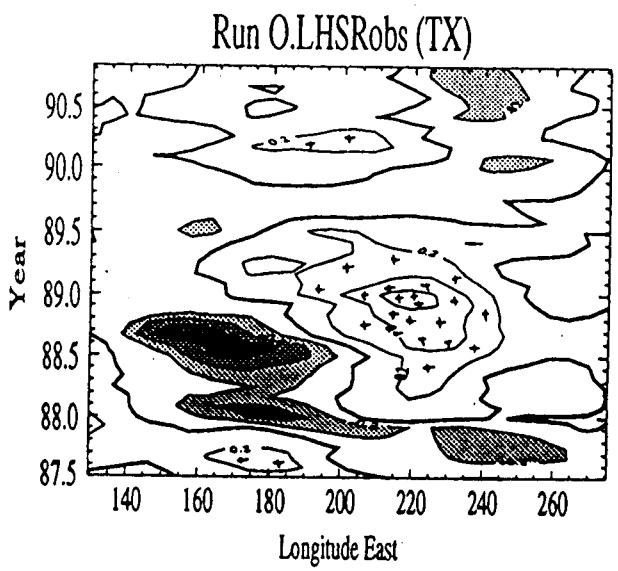
Run O.LHSRobs (TX)
Year
90.5
90.0
89.5
89.0
88.5
88.0
87.5
140
160
180
200
220
240
260
Longitude East

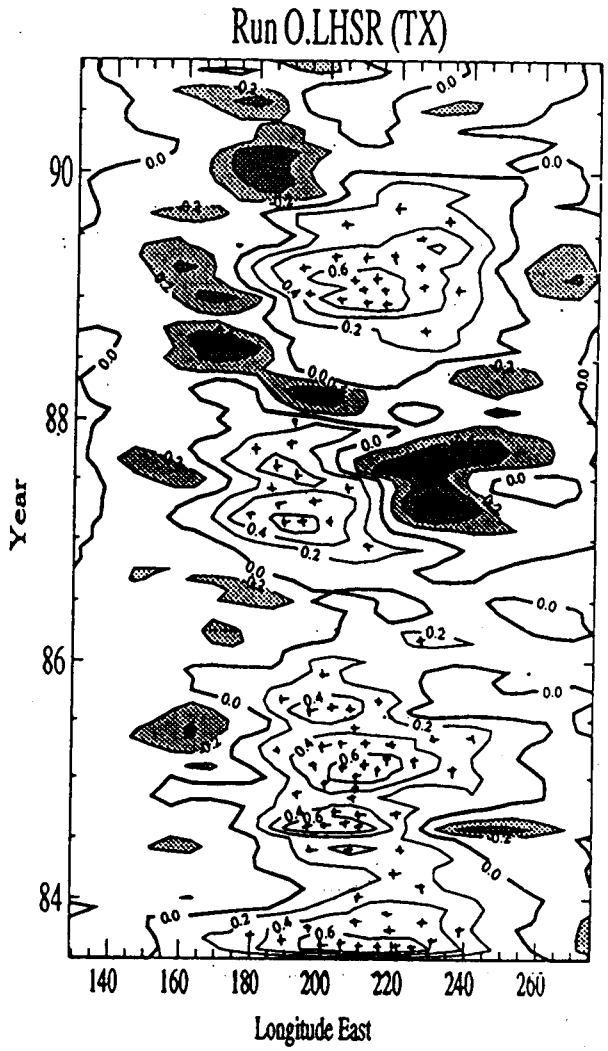
Run O.LHSR (TX)
Year
90
88
86
84
140
160
180
200
220
240
260
Longitude East

Fig. 12 a b

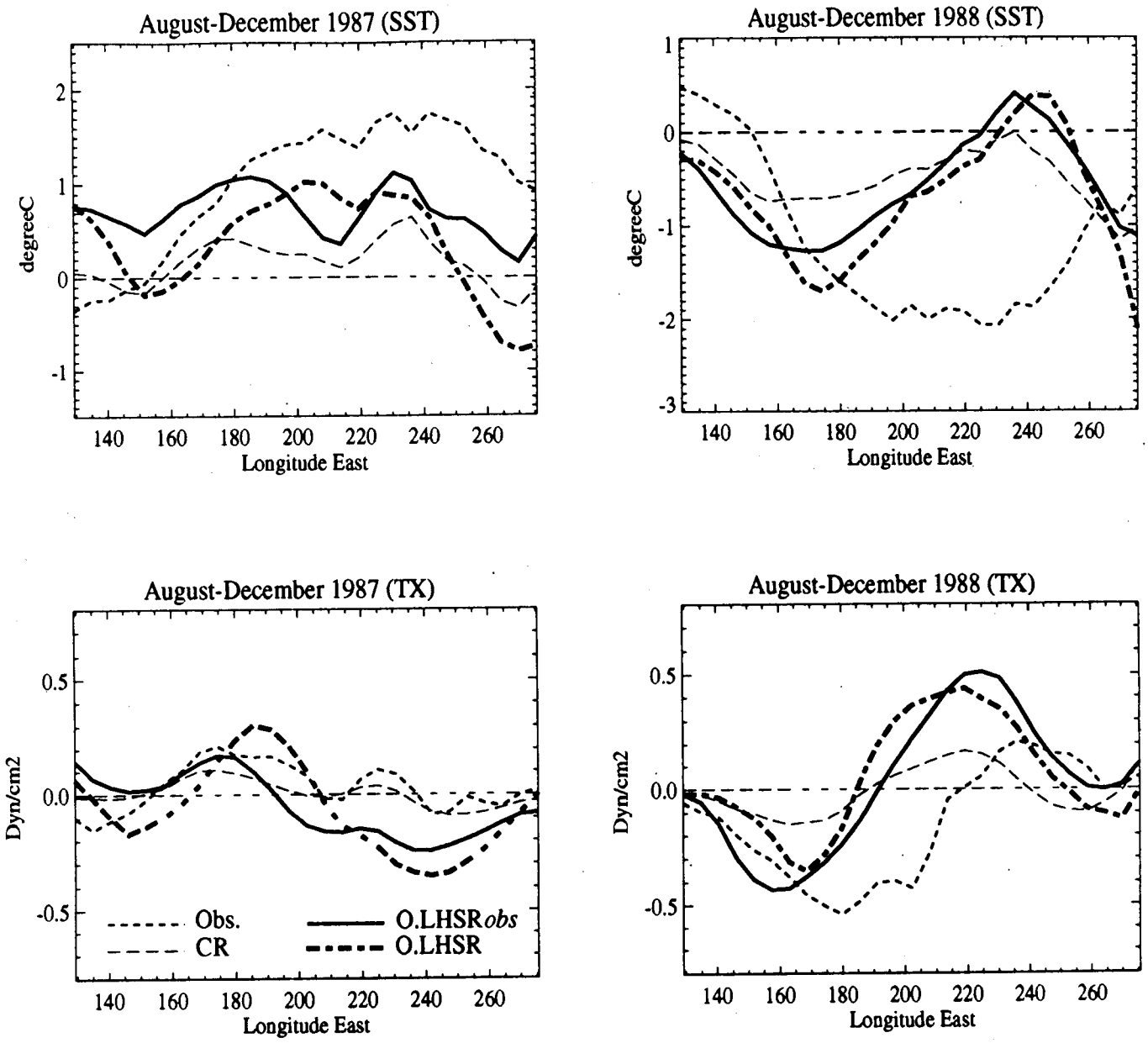
August-December 1987 (SST)
degreeC
Longitude East
August-December 1988 (SST)
degreeC
Longitude East
August-December 1987 (TX)
Dyn/cm2
Longitude East
Obs.
CR
O.LHSRobs
O.LHSR
August-December 1988 (TX)
Dyn/cm2
Longitude East

Fig. 13abcd

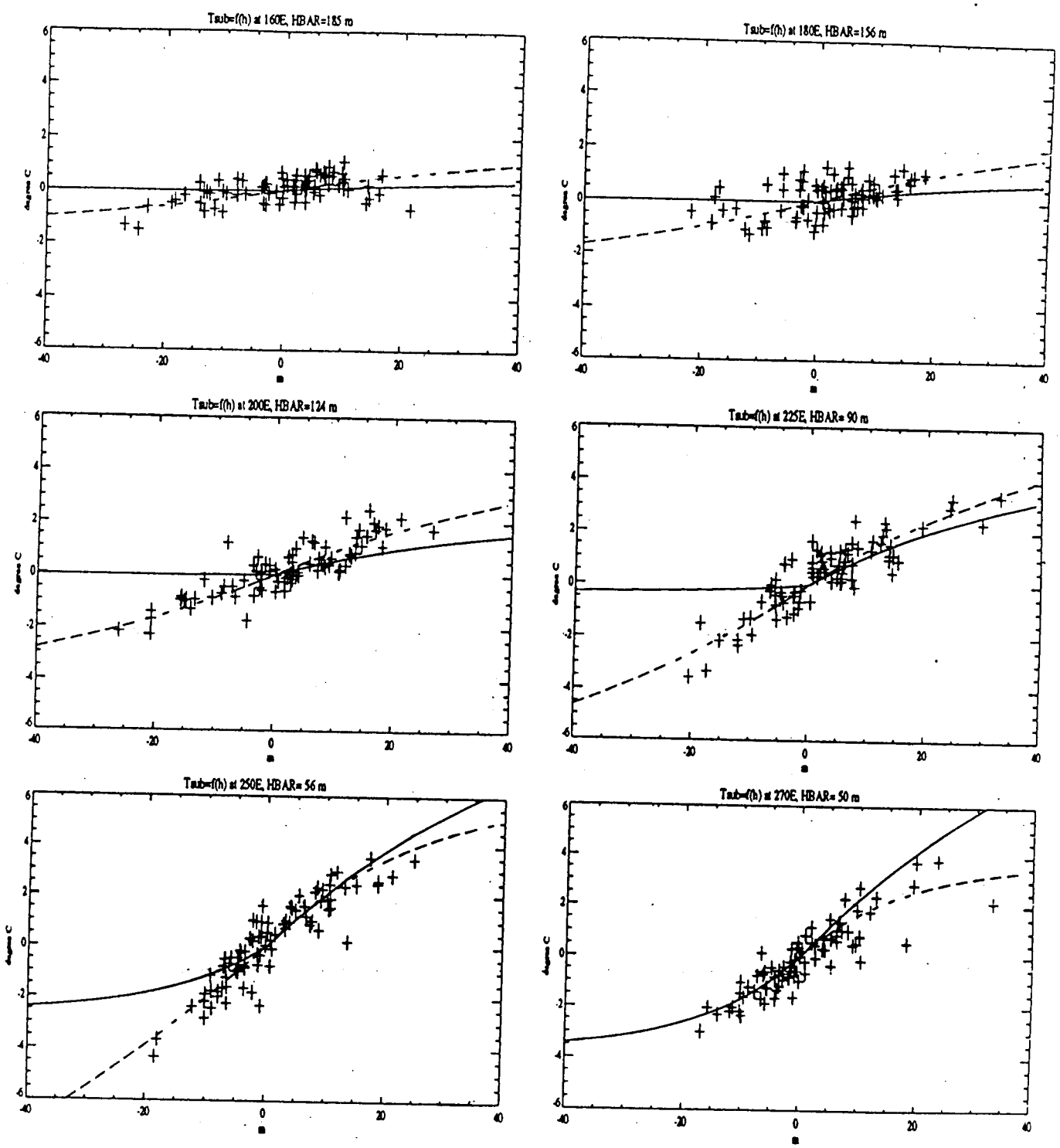


——— CR, +++ XBT data, - - - - Best fit.

Fig. 14

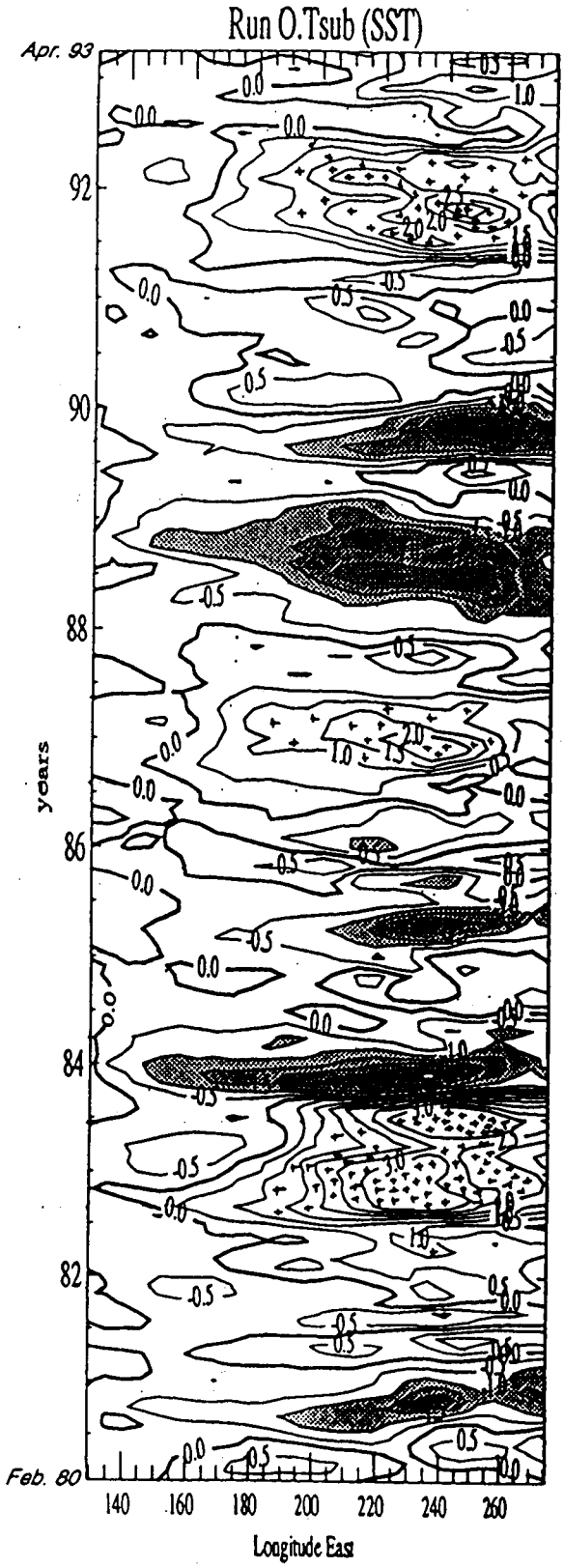
Run O.Tsub (SST)
Apr. 93
Feb. 80
years
92
90
88
86
84
82
140
160
180
200
220
240
260
Longitude East

Fig. 15a

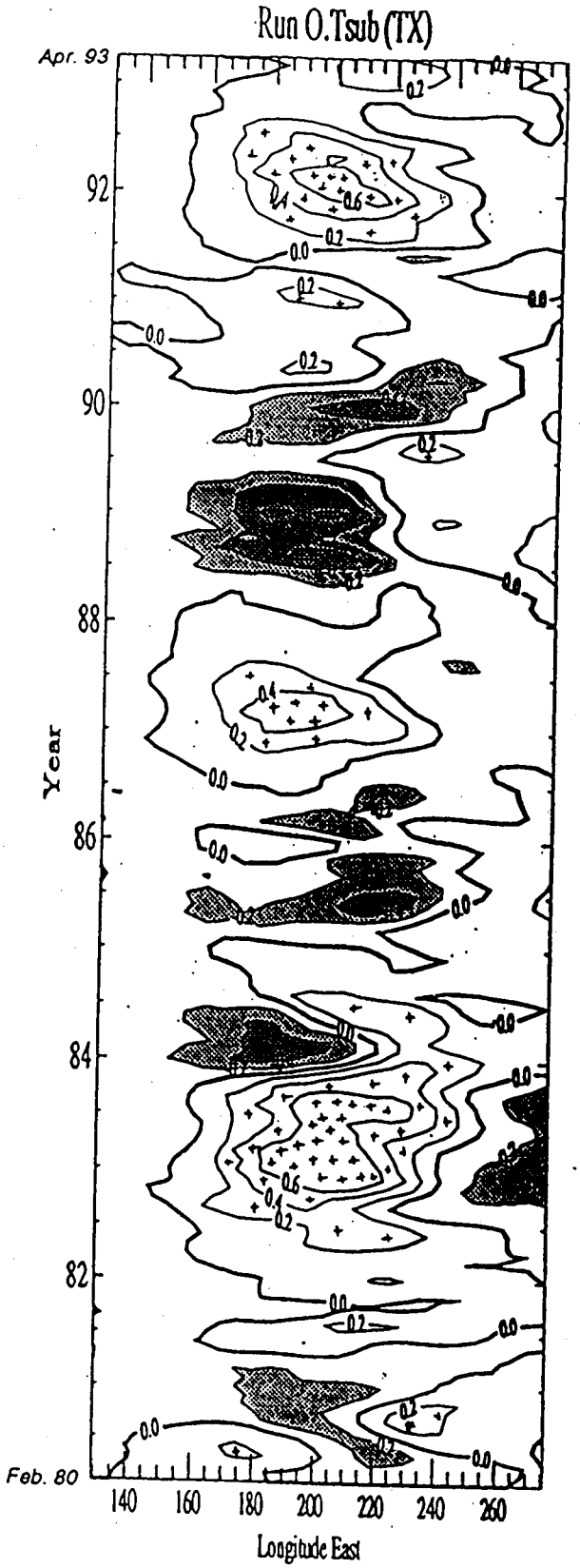
Run O.Tsub (TX)
Apr. 93
92
90
88
86
84
82
Feb. 80
Year
140
160
180
200
220
240
260
Longitude East

Fig. 15b

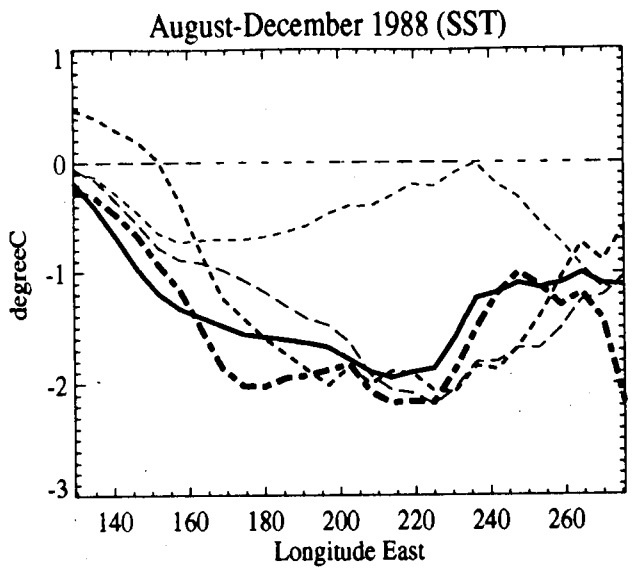
August-December 1988 (SST)
degreeC
1
0
-1
-2
-3
140
160
180
200
220
240
260
Longitude East

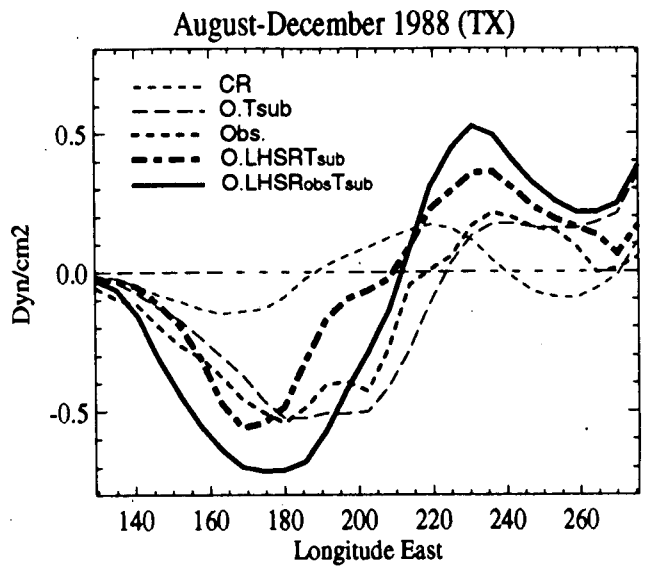
August-December 1988 (TX)
CR
O.Tsub
Obs.
O.LHSRTsub
O.LHSRobsTsub
Dyn/cm2
0.5
0.0
-0.5
140
160
180
200
220
240
260
Longitude East

Fig. 16ab

**Table 1a** : *Correlation and RMS of* ***zonal wind stress*** *(Apr. 85-Sep. 89).*

| | CORRELATION | | RMS (Dyn/cm2) | | RMSDIFF (Dyn/cm2) | |
|---|---|---|---|---|---|---|
| *Index* | NINO4 | NINO34 | NINO4 | NINO34 | NINO4 | NINO34 |
| FSU | 1.0 | 1.0 | 0.19 | 0.14 | 0.0 | 0.0 |
| CR | 0.67 | 0.45 | 0.10 | 0.09 | 0.15 | 0.13 |
| A.SST | 0.83 | 0.80 | 0.27 | 0.26 | 0.16 | 0.17 |
| A.SST0 | 0.81 | 0.80 | 0.22 | 0.22 | 0.11 | 0.10 |
| A.CVN0 | 0.27 | - 0.79 | 0.15 | 0.17 | 0.21 | 0.30 |
| A.SSTCVN | 0.74 | 0.62 | 0.23 | 0.10 | 0.16 | 0.11 |
| O.U1 | 0.75 | 0.53 | 0.13 | 0.13 | 0.13 | 0.13 |
| O.LHSR | 0.38 | - 0.31 | 0.14 | 0.18 | 0.19 | 0.26 |
| O.Tsub | 0.88 | 0.75 | 0.22 | 0.17 | 0.10 | 0.11 |
| O.Tsuby | 0.88 | 0.73 | 0.21 | 0.16 | 0.10 | 0.11 |
| O.LHSRTsub | 0.80 | 0.06 | 0.18 | 0.12 | 0.13 | 0.13 |

**Table 1b** : *Correlation and RMS of* ***meridional wind stress*** *(Apr. 85-Sep. 89).*

| | CORRELATION | | RMS (Dyn/cm2) | | RMSDIFF (Dyn/cm2) | |
|---|---|---|---|---|---|---|
| *Index* | NINO4N | NINO34N | NINO4N | NINO34N | NINO4N | NINO34N |
| FSU | 1.0 | 1.0 | 0.13 | 0.14 | 0.0 | 0.0 |
| CR | 0.24 | 0.29 | 0.03 | 0.04 | 0.13 | 0.14 |
| A.SST | 0.49 | 0.65 | 0.10 | 0.10 | 0.12 | 0.11 |
| A.SST0 | 0.57 | 0.69 | 0.07 | 0.09 | 0.11 | 0.10 |
| A.CVN0 | 0.68 | 0.44 | 0.16 | 0.12 | 0.12 | 0.14 |
| A.CVNSST | 0.73 | 0.72 | 0.13 | 0.12 | 0.10 | 0.10 |
| O.U1 | 0.10 | 0.11 | 0.03 | 0.05 | 0.13 | 0.15 |
| O.LHSR | - 0.30 | - 0.31 | 0.07 | 0.08 | 0.17 | 0.19 |
| O.Tsub | 0.38 | 0.44 | 0.05 | 0.06 | 0.12 | 0.13 |
| O.Tsuby | 0.36 | 0.37 | 0.04 | 0.06 | 0.12 | 0.13 |
| O.LHSRTsub | - 0.25 | - 0.14 | 0.06 | 0.07 | 0.15 | 0.17 |
| *Index* | NINO4S | NINO34S | NINO4S | NINO34S | NINO4S | NINO34S |
| FSU | 1.0 | 1.0 | 0.08 | 0.07 | 0.0 | 0.0 |
| CR | 0.38 | 0.32 | 0.03 | 0.03 | 0.07 | 0.06 |
| A.SST | 0.68 | 0.33 | 0.10 | 0.10 | 0.08 | 0.10 |
| A.SST0 | 0.70 | 0.34 | 0.06 | 0.06 | 0.06 | 0.07 |
| A.CVN0 | 0.52 | 0.30 | 0.09 | 0.11 | 0.08 | 0.11 |
| A.CVNSST | 0.73 | 0.39 | 0.08 | 0.10 | 0.06 | 0.09 |
| O.U1 | 0.66 | 0.47 | 0.05 | 0.04 | 0.06 | 0.06 |
| O.LHSR | 0.53 | 0.17 | 0.15 | 0.13 | 0.12 | 0.13 |
| O.Tsub | 0.63 | 0.49 | 0.06 | 0.06 | 0.06 | 0.06 |
| O.Tsuby | 0.64 | 0.49 | 0.07 | 0.06 | 0.06 | 0.06 |
| O.LHSRTsub | 0.60 | 0.30 | 0.17 | 0.14 | 0.13 | 0.13 |

**Table 2** : *Correlation and RMS of **SST** over the period Apr. 85-Sep. 89.*

| | CORRELATION | | | RMS (°C) | | | RMSDIFF (°C) | | |
|---|---|---|---|---|---|---|---|---|---|
| *Index* | NINO4 | NINO34 | NINO3 | NINO4 | NINO34 | NINO3 | NINO4 | NINO34 | NINO3 |
| AVHRR | 1 | 1 | 1 | 0.64 | 0.92 | 0.93 | 0 | 0 | 0 |
| CR | 0.79 | 0.65 | 0.56 | 0.34 | 0.46 | 0.52 | 0.43 | 0.71 | 0.77 |
| O.U1 | 0.67 | 0.55 | 0.56 | 0.40 | 0.60 | 0.71 | 0.48 | 0.77 | 0.79 |
| O.LHSR | 0.91 | 0.83 | 0.55 | 0.57 | 0.72 | 0.53 | 0.27 | 0.51 | 0.77 |
| O.Tsub | 0.84 | 0.84 | 0.79 | 0.54 | 0.82 | 0.85 | 0.35 | 0.50 | 0.58 |
| O.Tsuby | 0.84 | 0.83 | 0.77 | 0.53 | 0.80 | 0.79 | 0.35 | 0.51 | 0.59 |
| O.LHSRTsub | 0.94 | 0.92 | 0.83 | 0.75 | 1.04 | 0.80 | 0.26 | 0.40 | 0.52 |

**Table A1** : *Correlation and RMS of* ***solar radiation*** *over the period Jul. 83-Aug. 91.*

| | CORRELATION | | | RMS (W/m2) | | | RMSDIFF (W/m2) | | |
|---|---|---|---|---|---|---|---|---|---|
| *Index* | NINO4N | NINO34N | NINO3N | NINO4N | NINO34N | NINO3N | NINO4N | NINO34N | NINO3N |
| SR(Obs.) | 1 | 1 | 1 | 12.87 | 10.37 | 8.32 | 0 | 0 | 0 |
| SR(Para.) | 0.89 | 0.84 | 0.52 | 11.53 | 9.43 | 7.74 | 6.15 | 5.70 | 7.87 |
| | | | | | | | | | |
| *Index* | NINO4 | NINO34 | NINO3 | NINO4 | NINO34 | NINO3 | NINO4 | NINO34 | NINO3 |
| SR(Obs.) | 1 | 1 | 1 | 14.65 | 11.00 | 6.80 | 0 | 0 | 0 |
| SR(Para.) | 0.94 | 0.89 | 0.56 | 14.73 | 9.20 | 4.36 | 4.96 | 5.01 | 5.68 |
| | | | | | | | | | |
| *Index* | NINO4S | NINO34S | NINO3S | NINO4S | NINO34S | NINO3S | NINO4S | NINO34S | NINO3S |
| SR(Obs.) | 1 | 1 | 1 | 14.52 | 10.65 | 4.96 | 0 | 0 | 0 |
| SR(para.) | 0.92 | 0.87 | 0.30 | 15.21 | 8.72 | 1.95 | 6.00 | 5.20 | 4.75 |

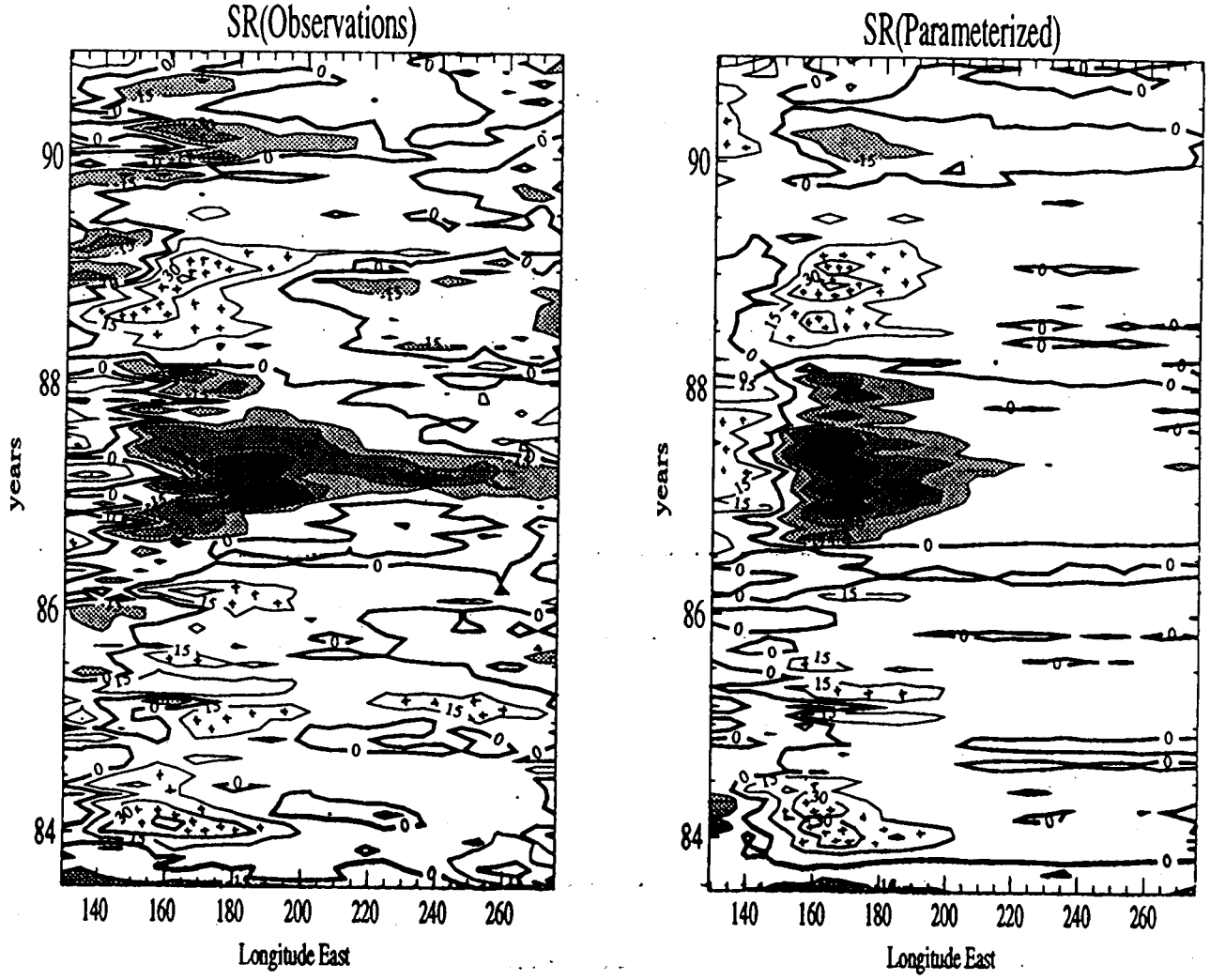
SR(Observations)
SR(Parameterized)
years
90
88
86
84
140
160
180
200
220
240
260
Longitude East

Fig. A1.1

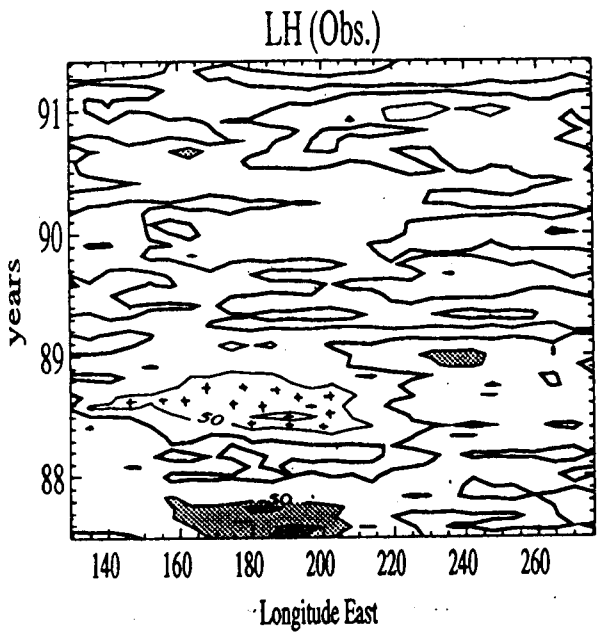


Fig. A2.1

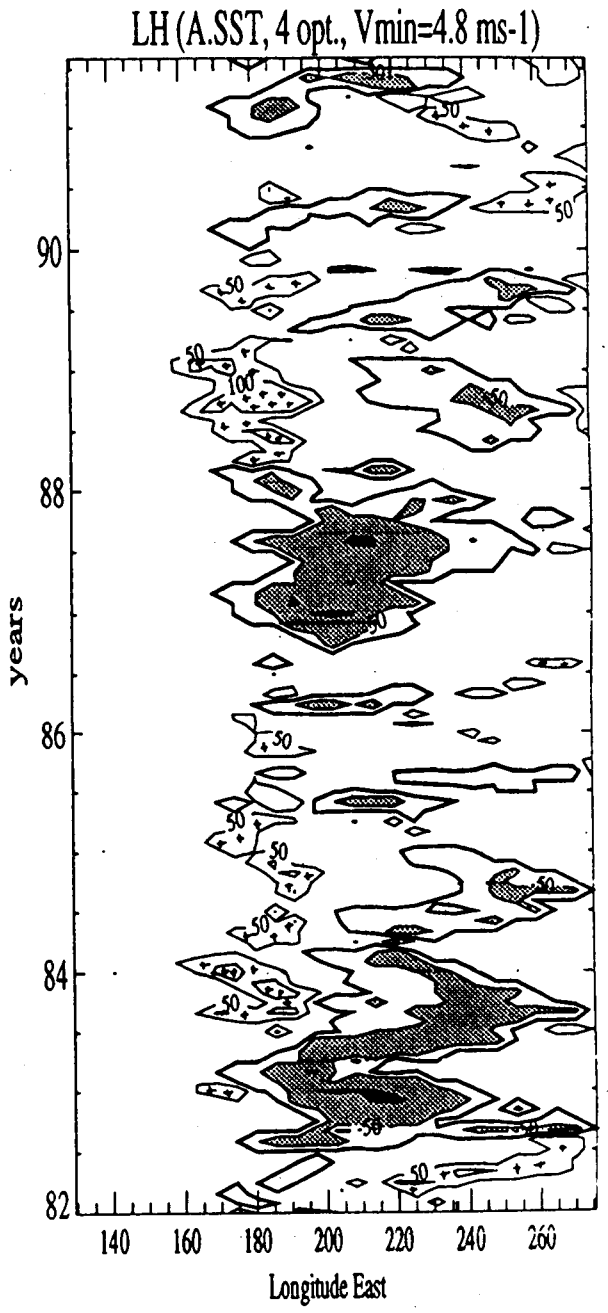


Fig. A2.2

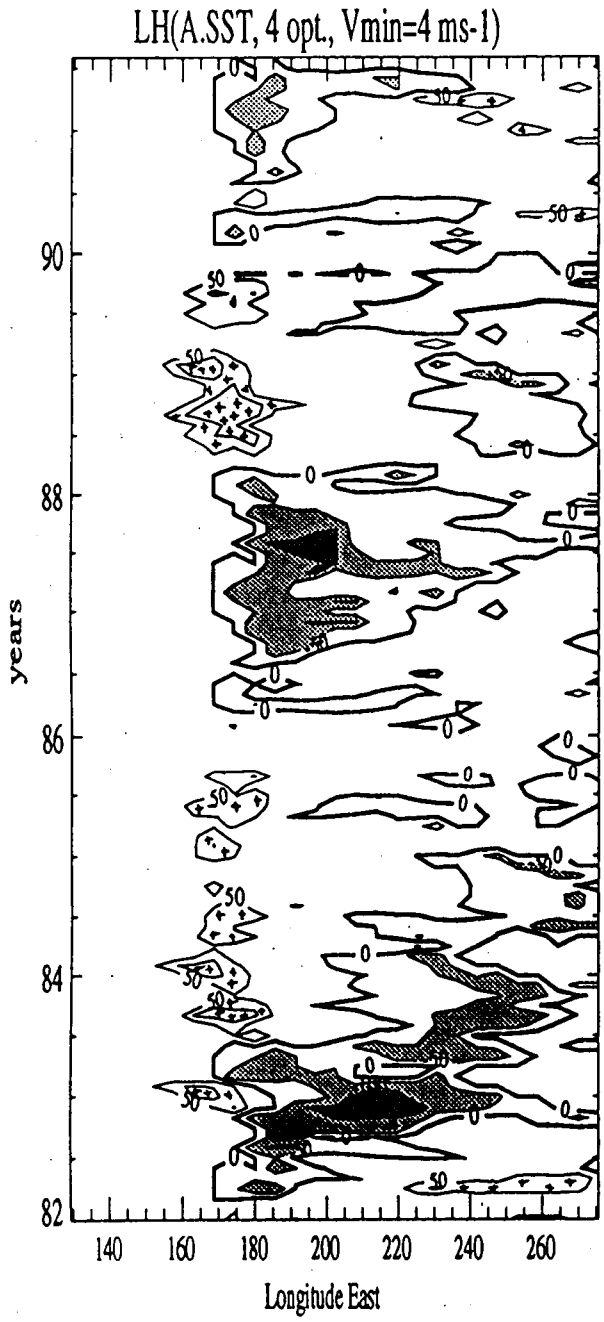


Fig. A2.3

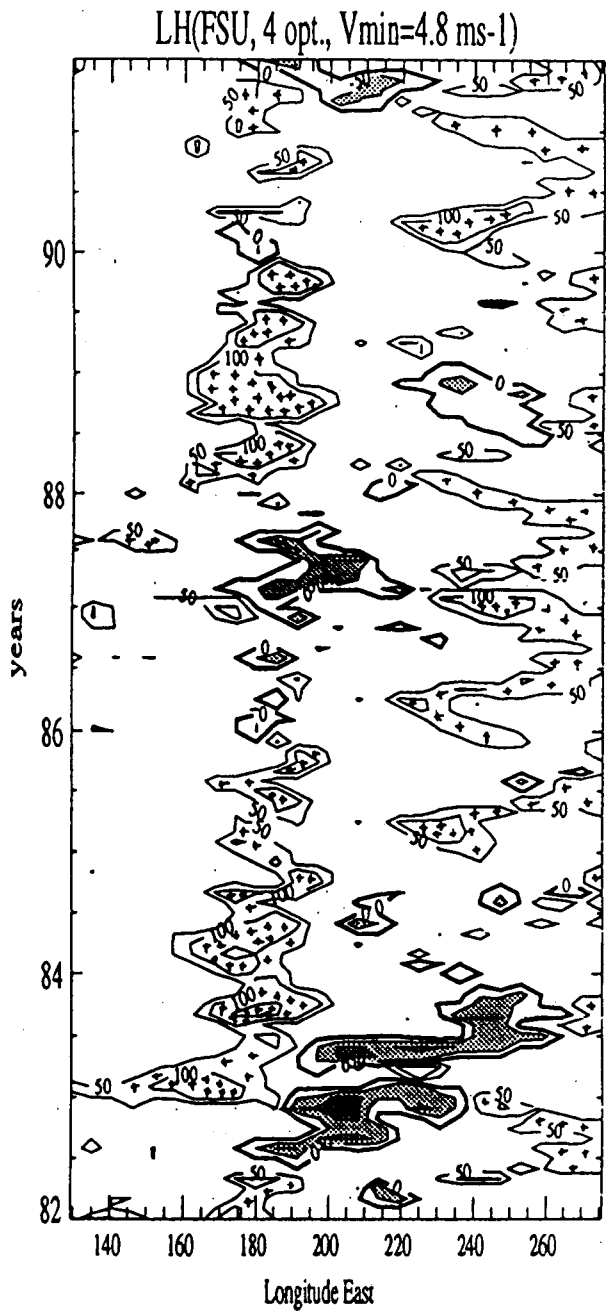


Fig. A2.4

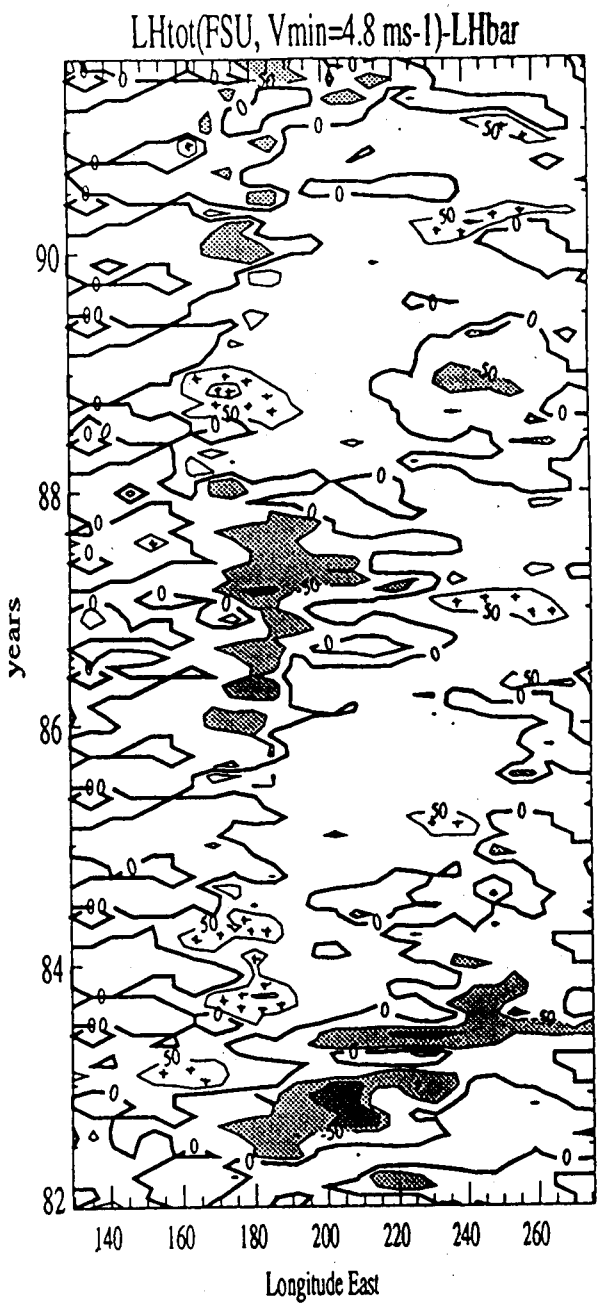


Fig. A2.5

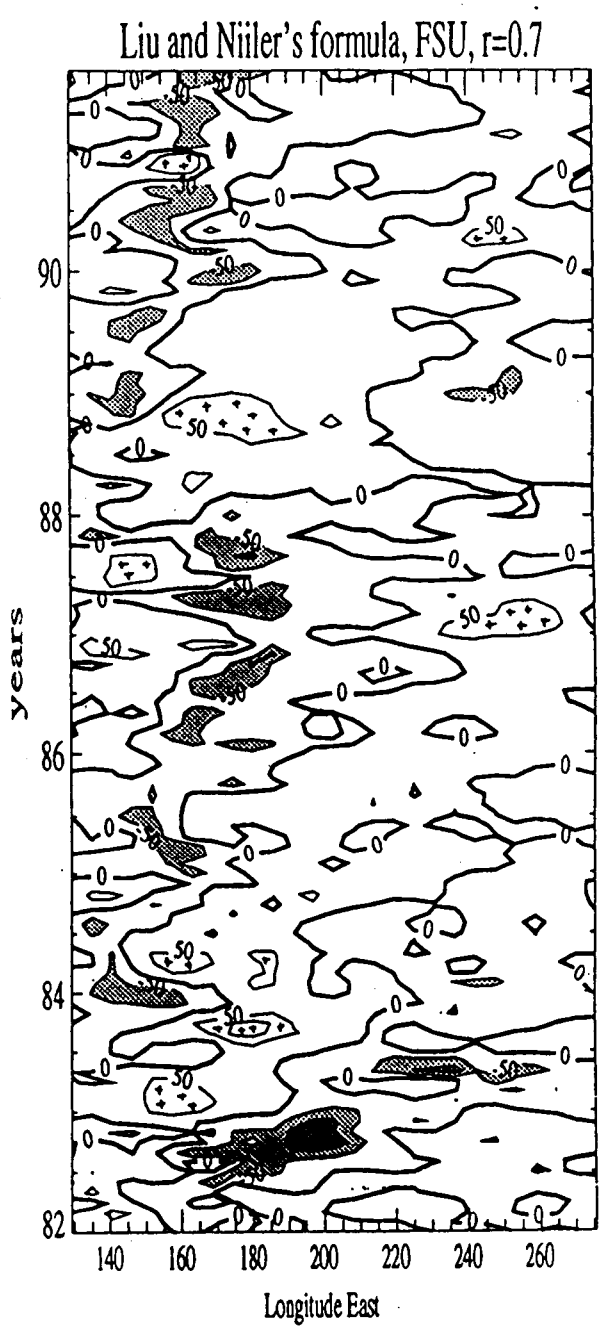


Fig. A2.6

**Table A2** : *Correlation and RMS of* ***Latent heat*** *over the period Jul. 87-Jun. 91.*

| | CORRELATION | | | RMS (W/m2) | | | RMSDIFF (W/m2) | | |
|---|---|---|---|---|---|---|---|---|---|
| *Index* | NINO4N | NINO34N | NINO3N | NINO4N | NINO34N | NINO3N | NINO4N | NINO34N | NINO3N |
| LH(Obs.) | 1 | 1 | 1 | 20.63 | 17.07 | 12.56 | 0 | 0 | 0 |
| A2.2 | 0.60 | 0.60 | 0.29 | 28.03 | 25.74 | 18.56 | 22.80 | 20.54 | 19.15 |
| A2.3 | 0.68 | 0.62 | 0.28 | 26.21 | 22.32 | 14.38 | 19.51 | 17.85 | 16.26 |
| A2.4 | 0.54 | 0.37 | 0.08 | 23.40 | 23.14 | 13.78 | 21.33 | 23.09 | 17.84 |
| A2.5 | 0.61 | 0.46 | 0.12 | 20.64 | 18.60 | 9.84 | 18.25 | 18.54 | 15.00 |
| A2.6 | 0.61 | 0.36 | 0.11 | 16.97 | 12.34 | 8.83 | 16.87 | 17.06 | 14.53 |
| *Index* | NINO4 | NINO34 | NINO3 | NINO4 | NINO34 | NINO3 | NINO4 | NINO34 | NINO3 |
| LH(Obs.) | 1 | 1 | 1 | 27.04 | 21.70 | 14.33 | 0 | 0 | 0 |
| A2.2 | 0.78 | 0.70 | 0.44 | 26.41 | 26.53 | 18.00 | 17.88 | 19.30 | 17.41 |
| A2.3 | 0.79 | 0.68 | 0.42 | 26.00 | 21.21 | 11.48 | 17.02 | 17.14 | 14.05 |
| A2.4 | 0.63 | 0.46 | 0.29 | 23.15 | 19.22 | 11.42 | 21.78 | 21.34 | 15.51 |
| A2.5 | 0.66 | 0.52 | 0.31 | 22.08 | 17.02 | 10.63 | 20.65 | 19.38 | 14.94 |
| A2.6 | 0.66 | 0.30 | 0.30 | 16.15 | 9.36 | 14.48 | 20.48 | 20.87 | 17.08 |
| *Index* | NINO4S | NINO34S | NINO3S | NINO4S | NINO34S | NINO3S | NINO4S | NINO34S | NINO3S |
| LH(Obs.) | 1 | 1 | 1 | 28.60 | 24.44 | 18.16 | 0 | 0 | 0 |
| A2.2 | 0.73 | 0.54 | 0.62 | 23.03 | 24.13 | 20.00 | 19.57 | 23.37 | 16.63 |
| A2.3 | 0.75 | 0.54 | 0.65 | 21.42 | 18.69 | 12.71 | 18.90 | 21.14 | 13.87 |
| A2.4 | 0.52 | 0.29 | 0.42 | 23.03 | 19.77 | 14.66 | 25.69 | 26.55 | 17.88 |
| A2.5 | 0.53 | 0.34 | 0.46 | 22.74 | 16.82 | 13.46 | 25.42 | 24.43 | 16.91 |
| A2.6 | 0.44 | - 0.02 | 0.40 | 16.38 | 9.97 | 17.67 | 25.89 | 26.59 | 19.66 |

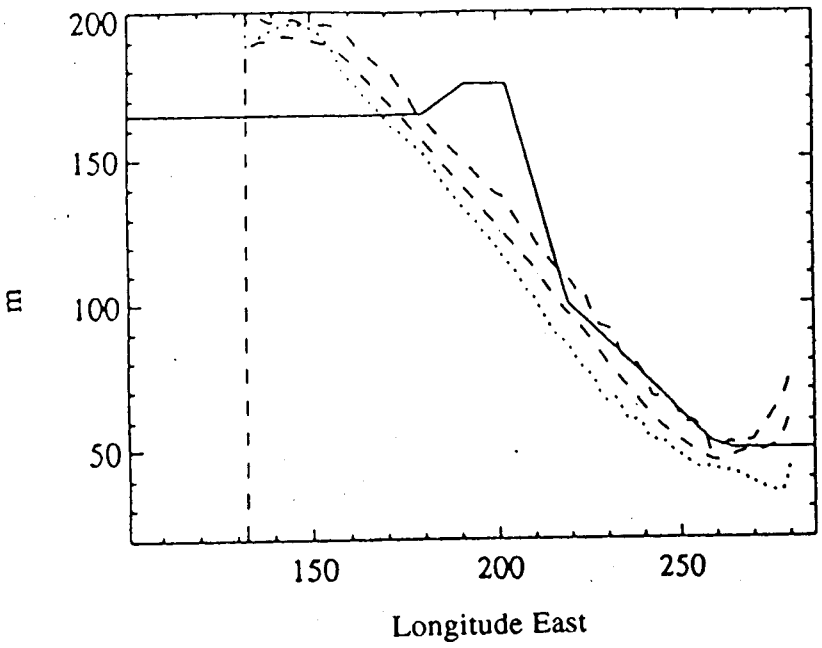


Fig. A3.1

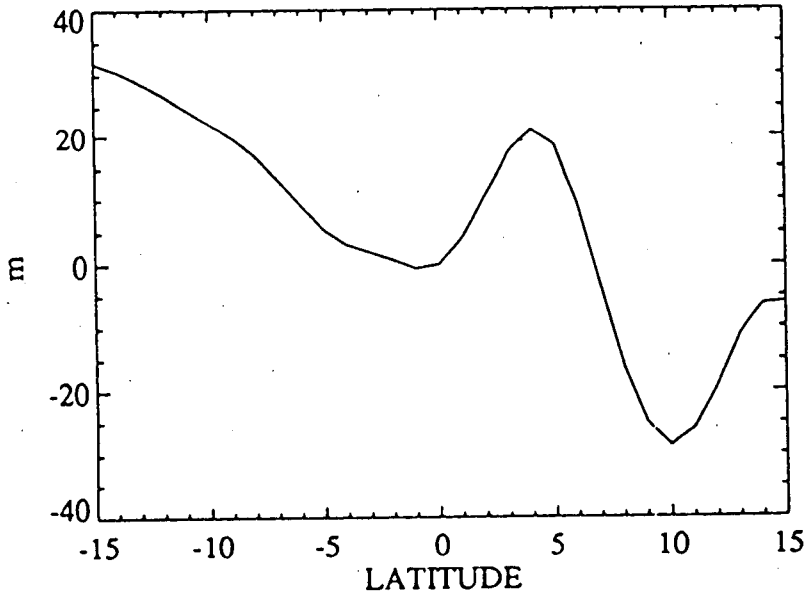


Fig A3.2